Fall 2018

Velocity Model for CO2 Sequestration in the Southeastern United States Atlantic Continental Margin

John Ollmann

VELOCITY MODEL FOR CO_2 SEQUESTRATION IN THE ATLANTIC CONTINENTAL MARGIN

by

John Ollmann

Bachelor of Science
University of Michigan, 2015

Submitted in Partial Fulfillment of the Requirements

For the Degree of Master of Science in

Geological Sciences

College of Arts and Sciences

University of South Carolina

2018

Accepted by:

Camelia C. Knapp, Director of Thesis

James H. Knapp, Reader

James N. Kellogg, Reader

Cheryl L. Addy, Vice Provost and Dean of the Graduate School

ACKNOWLEDGEMENTS

I would like to thank Camelia Knapp for believing in me and giving me the opportunity to join her lab. Her unwavering support throughout my time at the University of South Carolina is extremely appreciated. Also, thank you to James Knapp and James Kellogg for always being there to help discuss the research project. These professors graciously devoted their time and helped me develop as a geophysicist and professional. In order to complete my research project, I used several university licenses for software gifted by various companies. Thank you to Schlumberger, Halliburton, CGG, and Mathworks for the generous license donations to the University of South Carolina. Your respective university licenses for *Petrel*, Landmark *SeisSpace*, *ProMAX*, *HampsonRussell*, and *MATLAB* were essential to complete this thesis. The seismic reflection and well data in the study area are provided by the United States Geological Survey and Bureau of Earth and Ocean Management database. To everyone in the Geophysical Exploration Lab, I thoroughly enjoyed working with you and our friendships. Thank you for your help and support. I would especially like to thank Darrell Terry. He spent countless hours helping me further understand geophysics and software packages. Lastly, I would like to thank my family for supporting my ambitions in geology.

ABSTRACT

The sequestration of carbon dioxide (CO_2) is emerging as a major player in offsetting anthropogenic greenhouse gas emissions. With 40% of the United States' anthropogenic CO_2 emissions originating in the southeast, characterizing potential CO_2 sequestration sites is vital to reducing the United States' emissions. The overall goal of this research project, funded by the Department of Energy, is to estimate the CO_2 storage potential for the Southeastern United States Atlantic Continental Margin. Previous studies find storage potential in the Atlantic continental margin. Up to 16 Gt and 175 Gt of storage potential are estimated for the Upper Cretaceous and Lower Cretaceous formations, respectively. Considering 5.2 Gt of CO_2 were emitted by the United States in 2016, substantial storage potential is present in the Southeastern United States Atlantic Continental Margin.

Stratigraphic units were picked in two-way-time depth and were converted to depths in feet. Seismic reflection horizons were extrapolated using well log data from the COST GE-1 well. An interpolated seismic section was created using these seismic horizons. A velocity model was created using previously published stacking velocities. Semblance analysis was used to pick stacking velocities on common midpoint gathers from selected pre-stack seismic lines. These velocity analysis points were used for quality control of the published stacking velocities. Stacking velocities were converted to interval velocities using Dix conversion. These interval velocities are used to create the velocity

model and calculate the depths of stratigraphic units in feet. Using this velocity model, the seismic reflection data can be converted to depth in order to estimate the thickness and storage potential of CO_2 reservoirs in the Southeastern United States Atlantic Continental Margin.

TABLE OF CONTENTS

Acknowledgements iii

Abstract iv

List of Figures vii

List of Abbreviations ix

Chapter 1: Introduction 1

Chapter 2: Geological Background 3

Chapter 3: Objective 7

Chapter 4: Data 8

Chapter 5: Hypotheses 18

Chapter 6: Methodology 20

Chapter 7: Discussion 35

Chapter 8: Future Improvements 53

Chapter 9: Conclusions 57

References 59

LIST OF FIGURES

Figure 2.1 Bathymetric contour map 5

Figure 2.2 Potential CO_2 reservoirs map 6

Figure 4.1 SOSRA region map 10

Figure 4.2 Study area map 11

Figure 4.3 2D seismic reflection coverage 12

Figure 4.4 2D view of refraction data points 13

Figure 4.5 3D view of refraction data points 14

Figure 4.6 Well locations...15

Figure 4.7 Pre-stack seismic reflection data coverage.......................................16

Figure 6.1 Wells and refraction data map 25

Figure 6.2 Semblance analysis example 26

Figure 6.3 Velocity analysis on line se-3-28 27

Figure 6.4 Interval velocity conversion display...28

Figure 6.5 Extract stacking velocity locations from velocity analyses.............29

Figure 6.6 Interval velocity example on seismic line 30

Figure 6.7 2D view of stacking velocity data points from .geo files 31

Figure 6.8 2D view of all stacking velocity data points 32

Figure 6.9 3D view of all stacking velocity data points 33

Figure 6.10 Initial interval velocity cube 34

Figure 7.1 2D view of anomalous velocity points 39

Figure 7.2 Quality control for anomalous data points 40

Figure 7.3 Velocity analysis on CDP 281 for line se-3-28 41

Figure 7.4 Final interval velocity cube 42

Figure 7.5 2D seismic line velocity profile..43

Figure 7.6 Depth conversion of a seismic line...44

Figure 7.7 Upper Cretaceous depth comparisons 45

Figure 7.8 Stratigraphic column of COST GE-1 well 46

Figure 7.9 Upper Cretaceous surface..47

Figure 7.10 Seafloor surface 48

Figure 7.11 Upper Cretaceous stratigraphic depth surface 49

Figure 7.12 Upper Cretaceous surface exceeding 2625 ft. depth 50

Figure 7.13 Lower Cretaceous stratigraphic depth surface 51

Figure 7.14 Lower Cretaceous surface exceeding 2625 ft. depth..52

Figure 8.1 CDP gather example..55

Figure 8.2 Velocity analysis example with poor semblance analysis results 56

LIST OF ABBREVIATIONS

AMCOR..Atlantic Margin Coring

BOEM..Bureau of Ocean Energy Management

CO_2..Carbon Dioxide

CCS...Carbon Capture and Storage

IOGCC..Interstate Oil and Gas Compact Commission

SSEB..Southern States Energy Board

TVD .... Total Vertical Depth

TWT..Two-Way-Time

USGS .... United States Geological Survey

CHAPTER 1

INTRODUCTION

Increasing carbon dioxide (CO_2) concentration in the Earth's atmosphere is causing global temperatures to rise. The consequences of this increase in CO_2 concentration, such as melting of ice caps and acidification of the oceans, could have dramatic impacts on society. As a result, carbon capture and storage (CCS) is being looked at as a major contributor to offset CO_2 emissions. The Sleipner project, operated by Norway in the North Sea since 1996, is a major CO_2 sequestration project that confirms the capability of CCS (Eiken et al., 2011). At Sleipner, 1 million metric tons of CO_2 are injected each year as a byproduct of natural gas production (Schrag, 2009). However, 10 billion metric tons of CO_2 were emitted from power plants in 2007 (Schrag, 2009). Power plant emissions make up one-third of the global carbon emissions (Schrag, 2009). CCS projects worldwide need to be able to capture at least 10 billion metric tons of CO_2 per year to offset power plant emissions. In the United States, the majority of CO_2 sequestration projects are related to enhanced oil recovery projects.

Storage of CO_2 requires the presence of a porous and permeable reservoir rock overlain by an impermeable cap. Offshore reservoirs need to be located at greater than 2625 ft (800 m) depth in order for the CO_2 to enter a supercritical phase. In the supercritical phase, CO_2 behaves more like a liquid than a gas, dramatically increasing its density. For the offshore Alabama and western Florida Panhandle, Hills and Pashin

(2010) estimated 170 Gt of CO_2 can be stored in the Miocene sandstone. Additionally, 30 Gt can be stored in the deeper Cretaceous formations. According to a task force created by the Southern States Energy Board (SSEB) and the Interstate Oil and Gas Compact Commission (IOGCC), there is no assessment of the offshore carbon storage potential of the Atlantic Seaboard for the southeastern U.S. (SSEB, 2013). Of the 5.2 Gt of CO_2 emitted by the United States in 2016, 1.8 Gt is from the electric power sector (Lindstrom, 2017). CO_2 emissions from the electric power sector are the easiest to capture because the power plants are fixed CO_2 sources, unlike cars. With 26% of anthropogenic CO_2 emissions in the United States are emitted in the southeast, the assessment of this region is vital to the success to CCS in the United States (Mitchell, 2013). While it is possible for onshore sites to be used for CCS, as is the case in western Texas for enhanced oil recovery, offshore sites offer advantages over onshore sites (Schrag, 2009). Federal ownership of offshore regions is advantageous. The increase in subsurface pressures as a result of the added CO_2 can cause pore fluids to be displaced from the formation. Onshore, these fluids commonly contain high concentrations of toxic metals (Schrag, 2009). Offshore, the pore fluid is similar to seawater, making the displacement of this pore fluid not harmful according to the EPA (Schrag, 2009).

CHAPTER 2

GEOLOGICAL BACKGROUND

The Atlantic continental margin begins with continental rifting in the Early Mesozoic. The rifting created extensional basins due to local tectonic subsidence. Beginning in the Jurassic and continuing to the present, thermal subsidence occurred on the eastern North American margin (Poag, 1991). The stratigraphy in the eastern North American margin is characterized by extensive lateral continuity and minimal structural disruption (Poag, 1991). Thick sequences of Jurassic to Pleistocene post-rift stratigraphy are present in the Mid-Atlantic and South Atlantic Continental Margin (Poag, 1991). Major sequences in the study area are the Carolina Trough, Southeast Georgia Embayment, and Blake Plateau (Figure 2.1). The thicknesses of sediment in these depocenters range from 10,000 to 25,000 ft (Maher and Applin, 1971). A post-rift unconformity lies below the post-rift sediments. This unconformity signifies the termination of rifting between Africa and North America and the beginning of the drift phase from 165-190 Ma (Poag, 1991).

Jurassic sediments are the oldest post-rift sediments. These sediments are characterized by rapid clastic sedimentation from erosion followed by evaporate and carbonate deposition (Dillon and Popenoe, 1988; Poag, 1991). Previous studies find the Jurassic sedimentary section thickens seawards and can reach a thickness of 7-8 km (Dillon et al., 1979). The Cretaceous section in the northern portion of the study area is characterized by clastic sedimentation while the southern portion contains more carbonate deposition. The Blake Plateau and offshore Florida contain a large Cretaceous carbonate platform.

Paleocurrents controlled sediment deposition from the late Cretaceous to the Cenozoic. In the late Cretaceous, the Suwannee Strait deposited clastic sediment to the Blake Plateau, creating a distinct facies change compared to the carbonates present in the Bahamas and offshore Florida (Pinet and Popenoe, 1985). Cenozoic stratigraphy in offshore Florida are dominated by carbonates, while Cenozoic deposits become more interbedded with limestone, limy shale, sandstone, and clay moving northward.

The major potential reservoirs in the study area are the Upper and Lower Cretaceous formations. Previous studies estimate storage capacities of 16 Gt and 175 Gt for these respective formations (Figure 2.2, Smyth et al., 2007). These potential CO_2 sinks need to be overlain by a low-permeability seal layer to be feasible for CO_2 storage. Also, the sinks must be porous and permeable to hold the CO_2. Porous sandstones in the interbedded Cenozoic deposits are the targets when searching for potential CO_2 reservoirs. Ideally, non-permeable shales will overly these sandstones to provide an effective trap and seal.

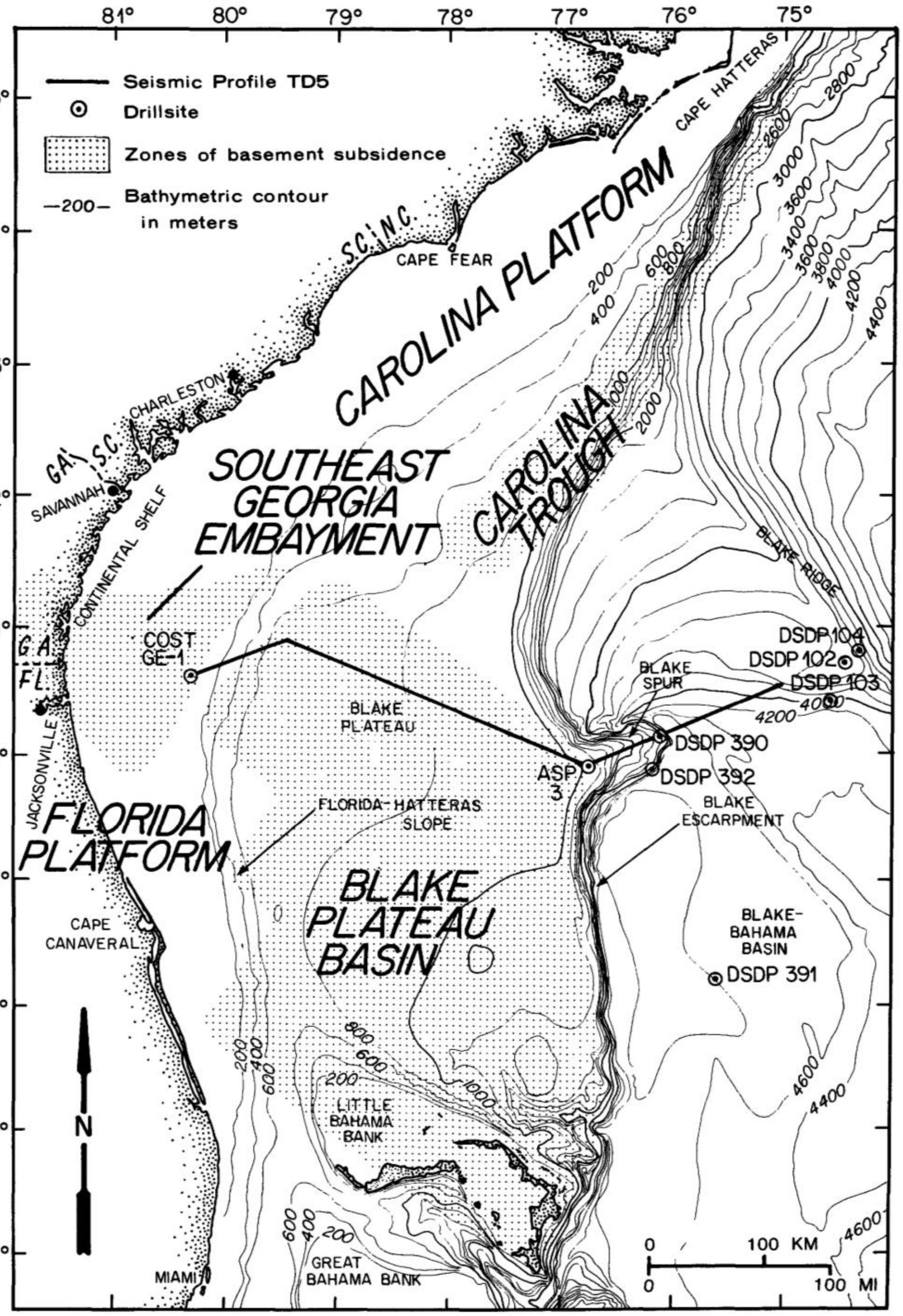

Figure 2.1: Bathymetric contour map of the Atlantic Continental Margin with major geological features labeled (Scholle, 1979)

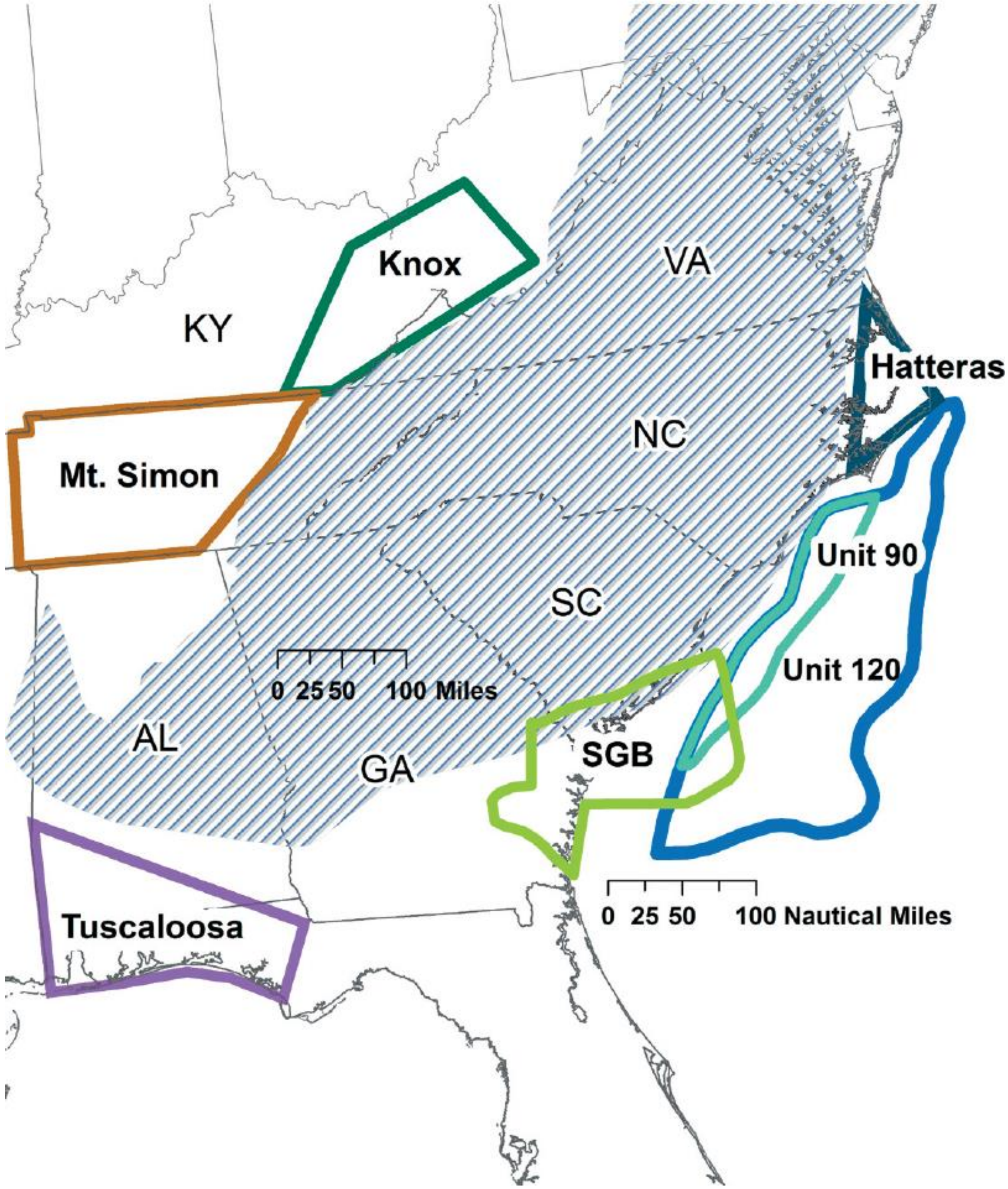

Figure 2.2: Potential CO_2 storage reservoirs are outlined. Unit 90 (Upper Cretaceous) and Unit 120 (Lower Cretaceous) have an estimated 16 Gt and 175 Gt of storage potential, respectively (Smyth et al., 2007).

CHAPTER 3

OBJECTIVE

The creation of the velocity model addresses two DOE Carbon Storage Program goals. This model will help accomplish the goal to "support industry's ability to predict CO_2 storage capacity in geologic formations to within ±30 percent." Also, a velocity model is beneficial to the development of a "Best Practice Manual," particularly for the site screening, selection, and initial characterization sections.

The main goal of this project is to create a velocity model using previously acquired seismic reflection and refraction data. This model can be used to create a 3D time-depth relationship for the seismic data in the study area to convert two-way travel time seismic sections to depth. The model more accurately estimates the stratigraphic depths and thicknesses on the Atlantic continental margin. Better estimates of reservoir thickness will yield more accurate CO_2 storage capacity estimates for the study area. Additionally, the depth converted formation surfaces will be useful in determining if potential reservoirs exceed the 2625 ft depth threshold for supercritical CO_2 storage.

CHAPTER 4

DATA

The SOSRA project focuses on offshore regions of the United States Atlantic Continental Margin (Figure 4.1). Oklahoma State University is assessing the Gulf of Mexico region while Virginia Polytechnic Institute and State University is assessing the Mid-Atlantic region. This particular project focuses on the South Atlantic offshore region that the University of South Carolina is working on (Figure 4.2). Public domain 2D reflection seismic surveys and geophysical well logs in the study area are available through the Bureau of Ocean Energy Management (BOEM) and United States Geological Survey (USGS) databases (Figure 4.3). The seismic surveys and geophysical data were used in previous projects to tie the seismic to well tops. The seismic data and its associated stacking velocity data points were used to create a 3D velocity model.

Hersey et al, 1959, Katz & Ewing, 1956, and Sheridan et al., 1966 provided refraction data with stratigraphic units picked. The refraction data points were acquired using 128 recording stations. 538 data points indicating stratigraphic units at various locations and depths were published (Figures 4.4 & 4.5). The refraction data points serve as control for the depths estimated when using the velocity model. Hersey et al., 1959 published tops of specific formations found in the refraction study. On the other hand, Katz & Ewing, 1956 and Sheridan et al., 1966 published more ambiguous data points for formations. In these 2 papers, the data points published are not tops, but rather points somewhere within the formation associated with each data point. 7 exploratory wells are present in the south Atlantic, most of which provide the following logs: Borehole Compensated Sonic Log, Compensated Formation Density Log, Compensated Neutron Formation Density, Computed Log, Continuous Diameter, Dual Laterolog, Temperature Log, and Sonic Log (Figure 4.6). For the COST GE-1 well, the USGS published a geological study in 1979 containing several key datasets such as velocity data and formation tops (Scholle, 1979). Five Atlantic Margin Coring (AMCOR) shallow wells are also present with a maximum depth of 308 m.

Pre-stack data acquired in 1975 by the Institute for Geophysics at the University of Texas at Austin provides an opportunity to perform velocity analysis. The velocity analysis points serve as further control on the velocity model. This pre-stack, unprocessed data for the southeast Georgia Embayment was acquired on cruise IG1501 (Figure 4.7). Table 4.2 lists further details of the acquisition parameters for this survey.

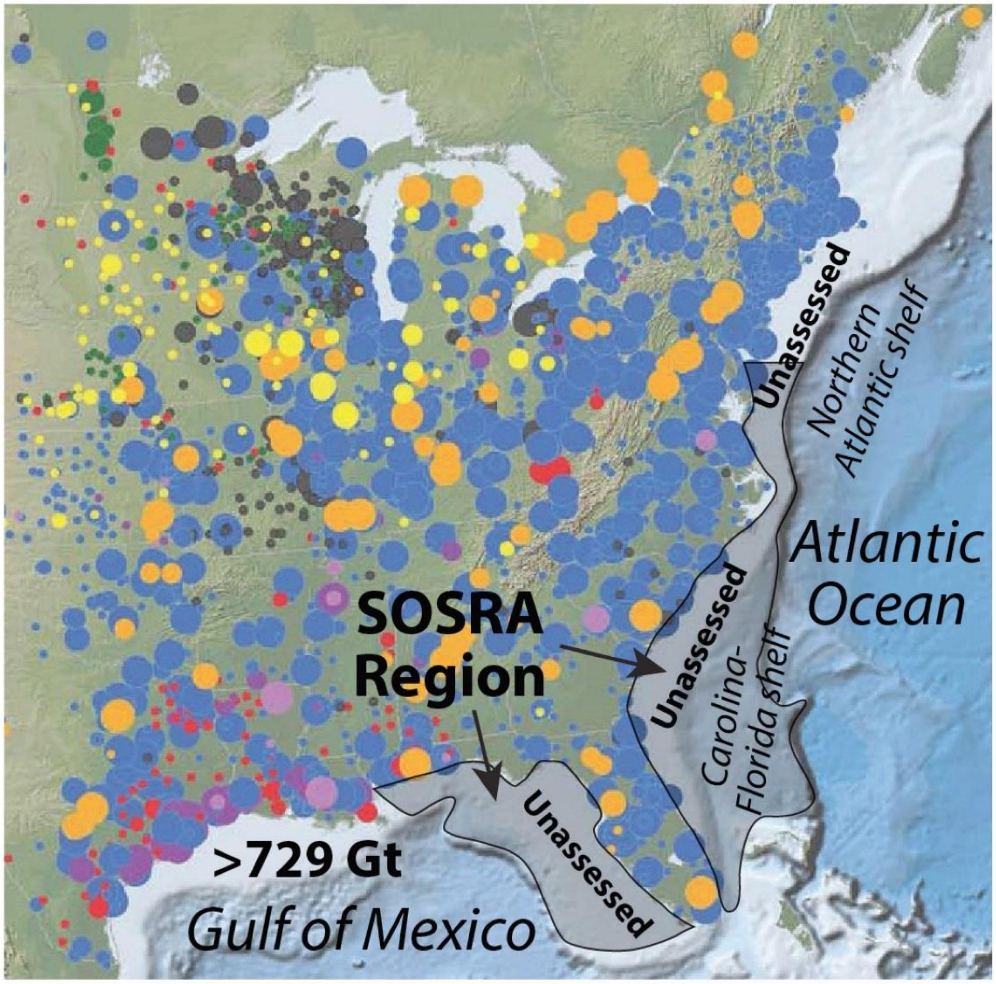

Figure 4.1: Location of the SOSRA region in relation to CO_2 point sources (SSEB, 2013; NETL, 2010)

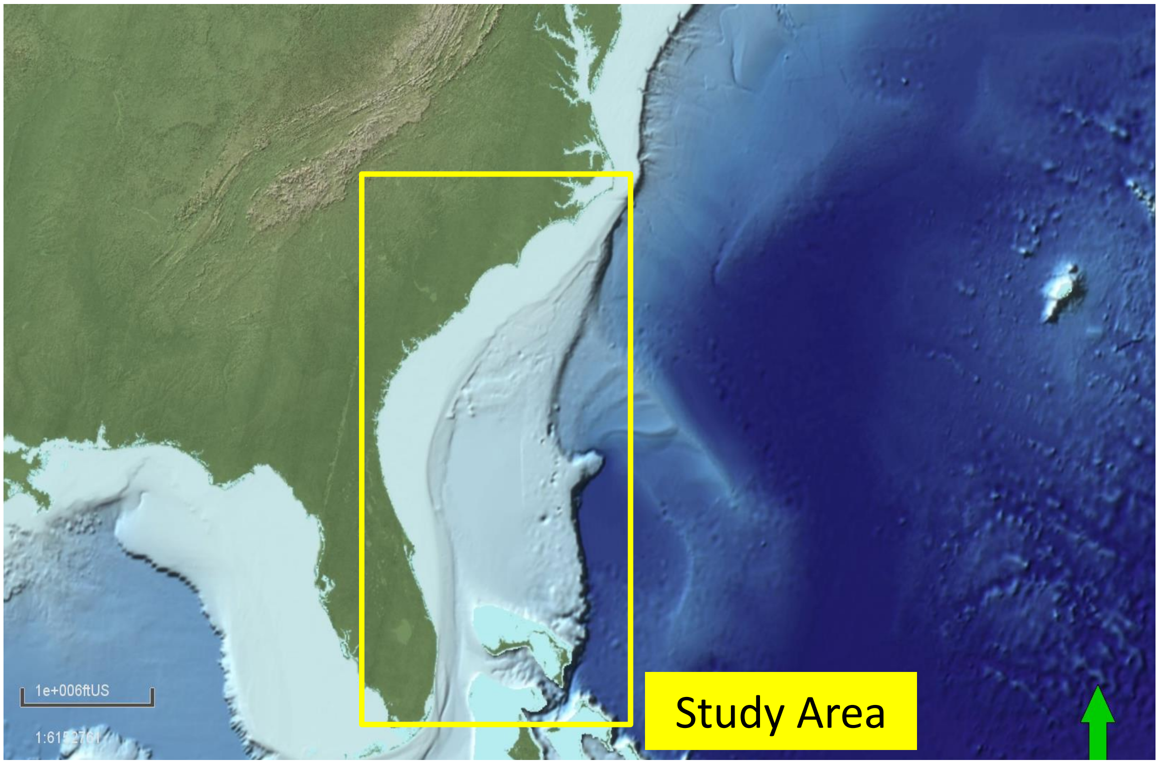

Figure 4.2: Location of the study area

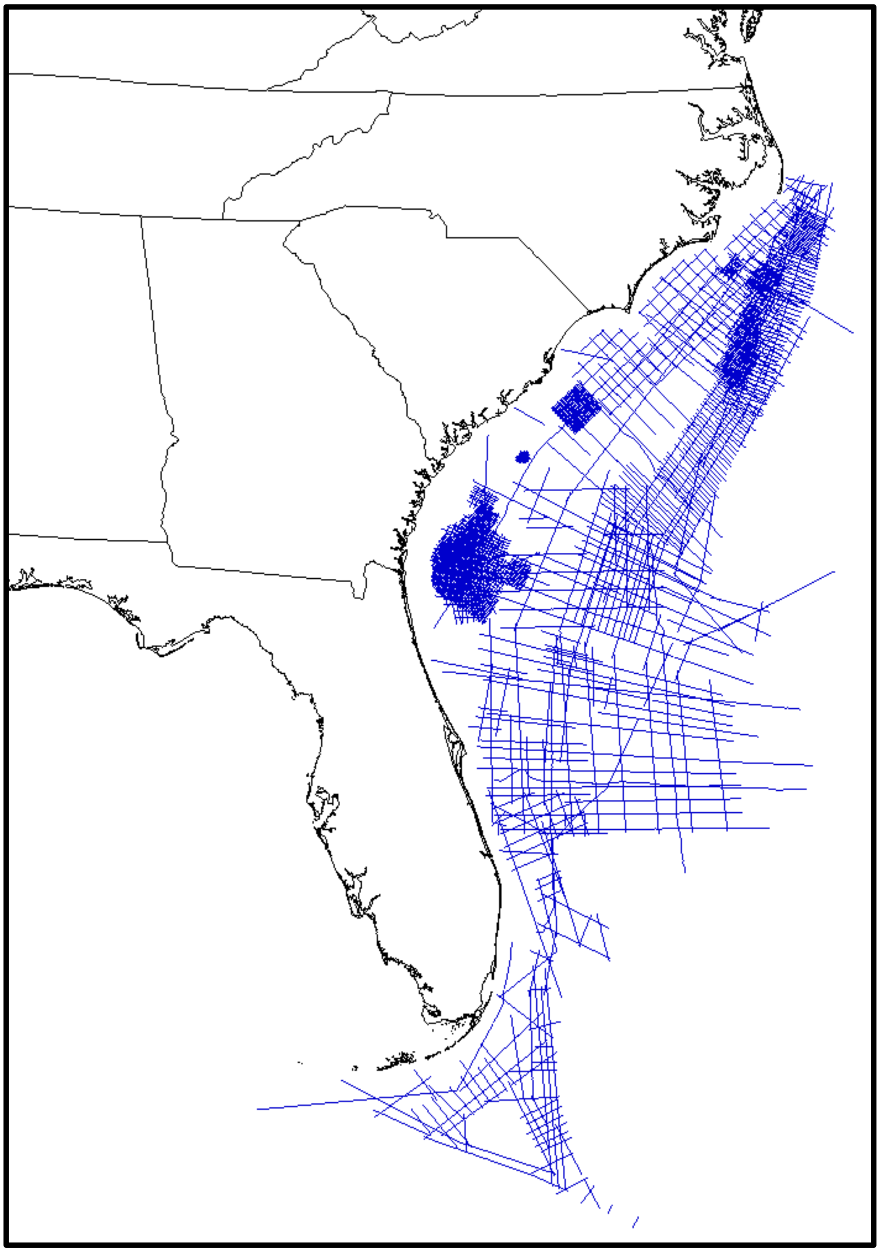

Figure 4.3: 2D seismic reflection data coverage

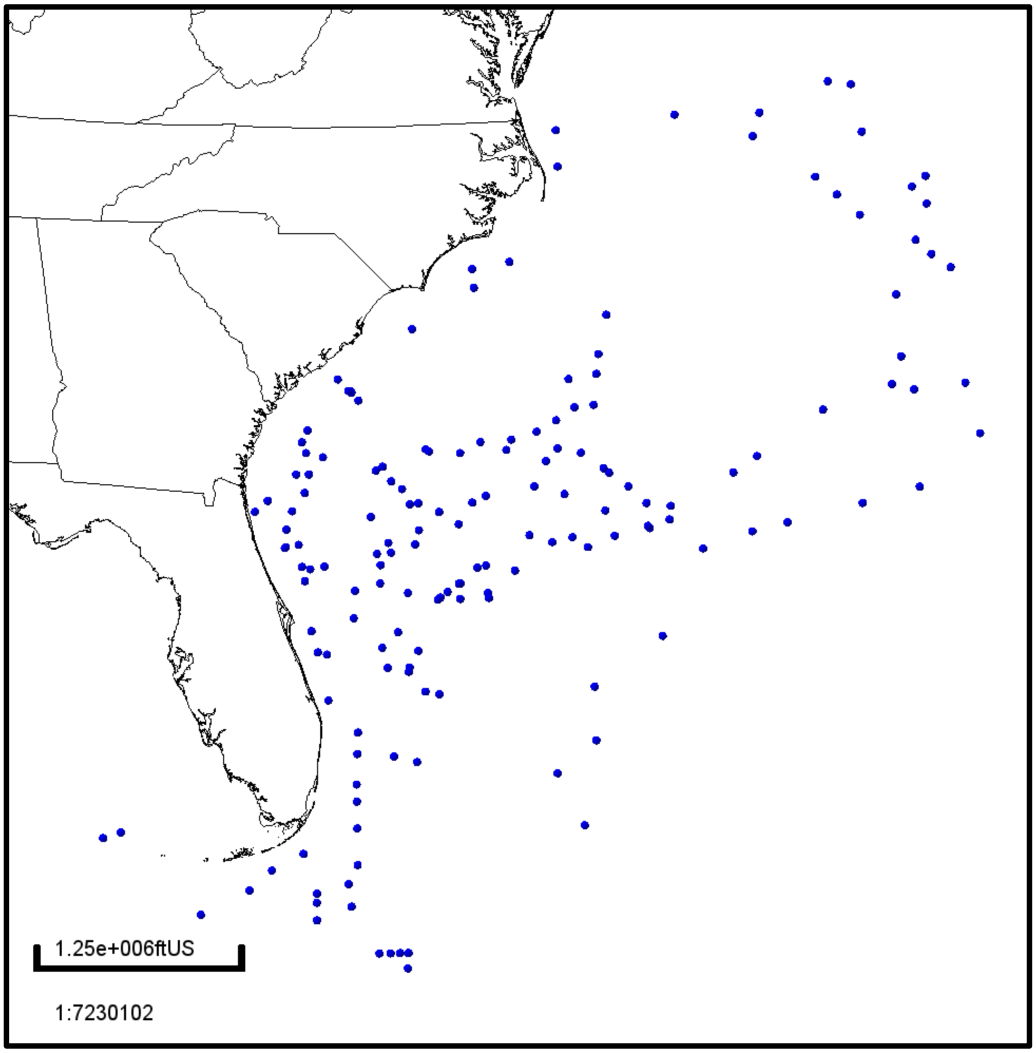

Figure 4.4: Data points from refraction studies (Hersey et al., 1959; Sheridan et al., 1966; Katz & Ewing, 1956)

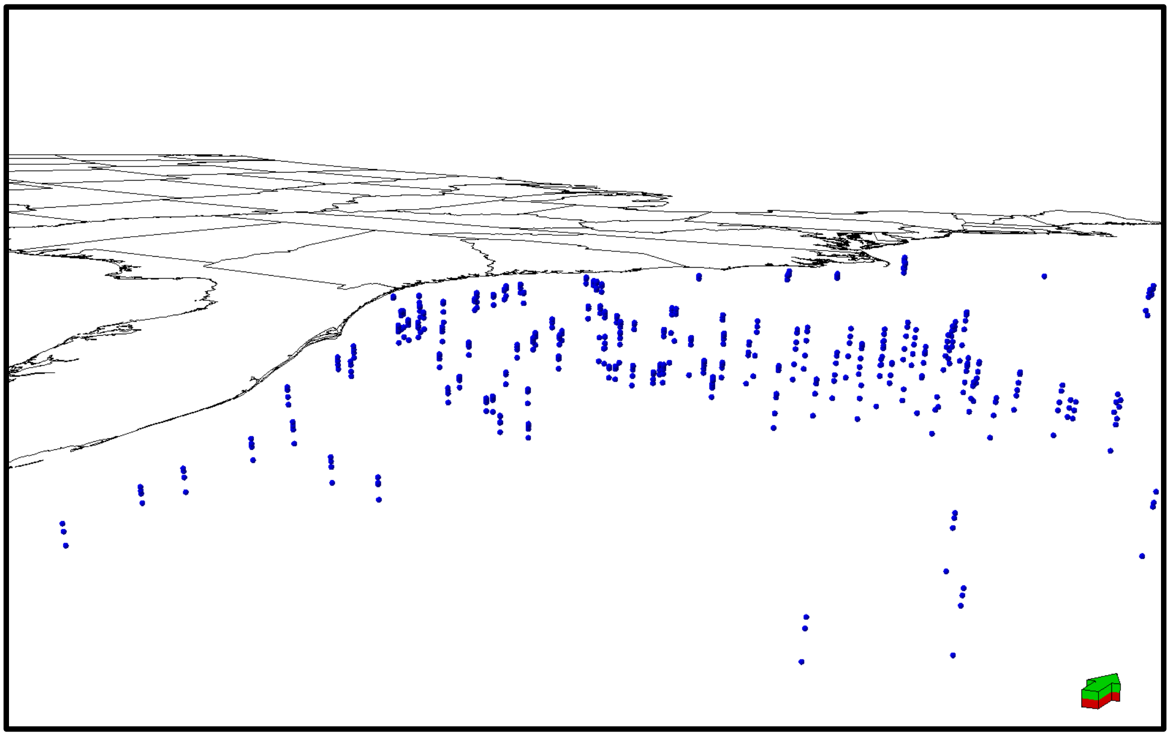

Figure 4.5: 3D view of refraction data points

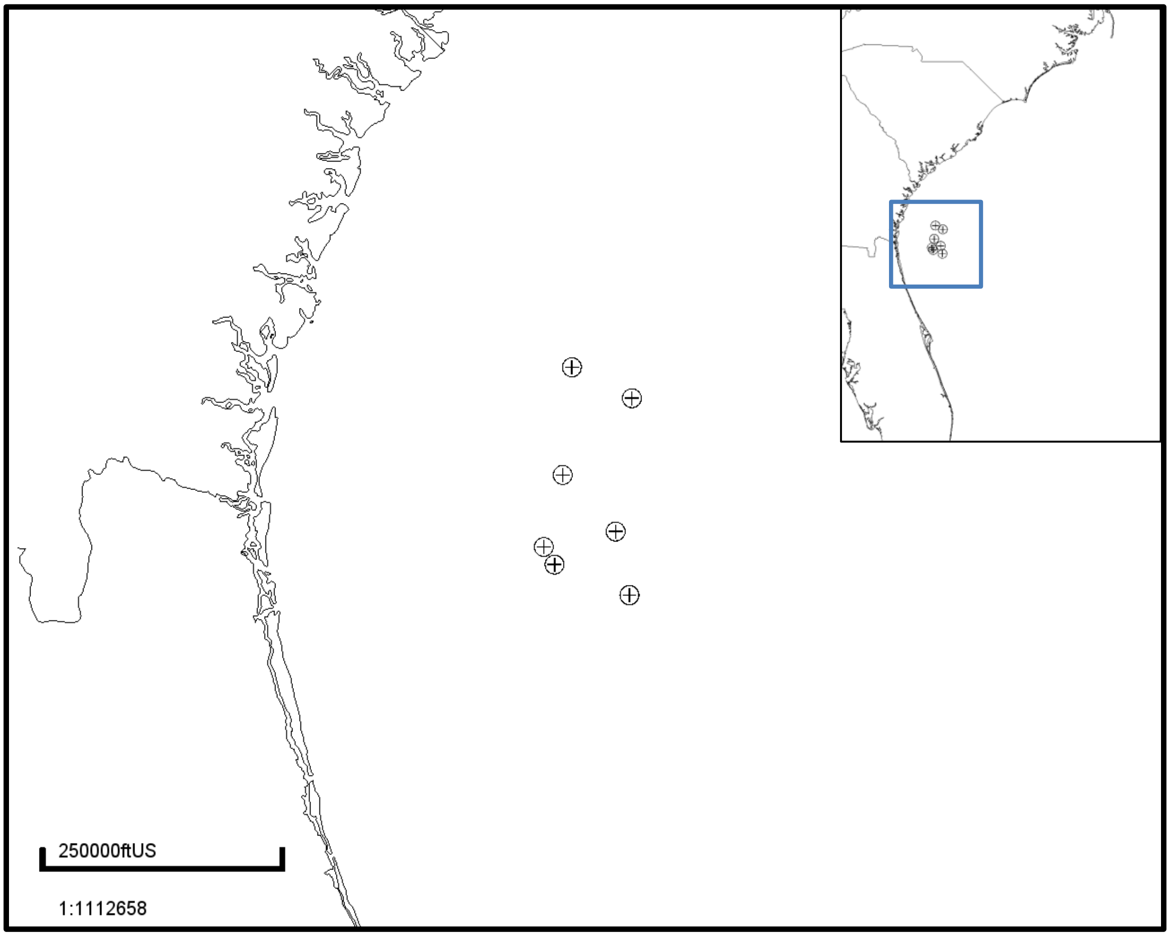

Figure 4.6: Locations of 7 exploration wells in the study area

Table 4.1: Total Vertical Depths of Selected Wells		
Well Name	**Water Depth (ft)**	**Total Vertical Depth (ft)**
913	109	7000
1005	134	11635
208	124	7754
COST GE-1	136	13254
427	98	7472
472	125	7758
564	145	12863

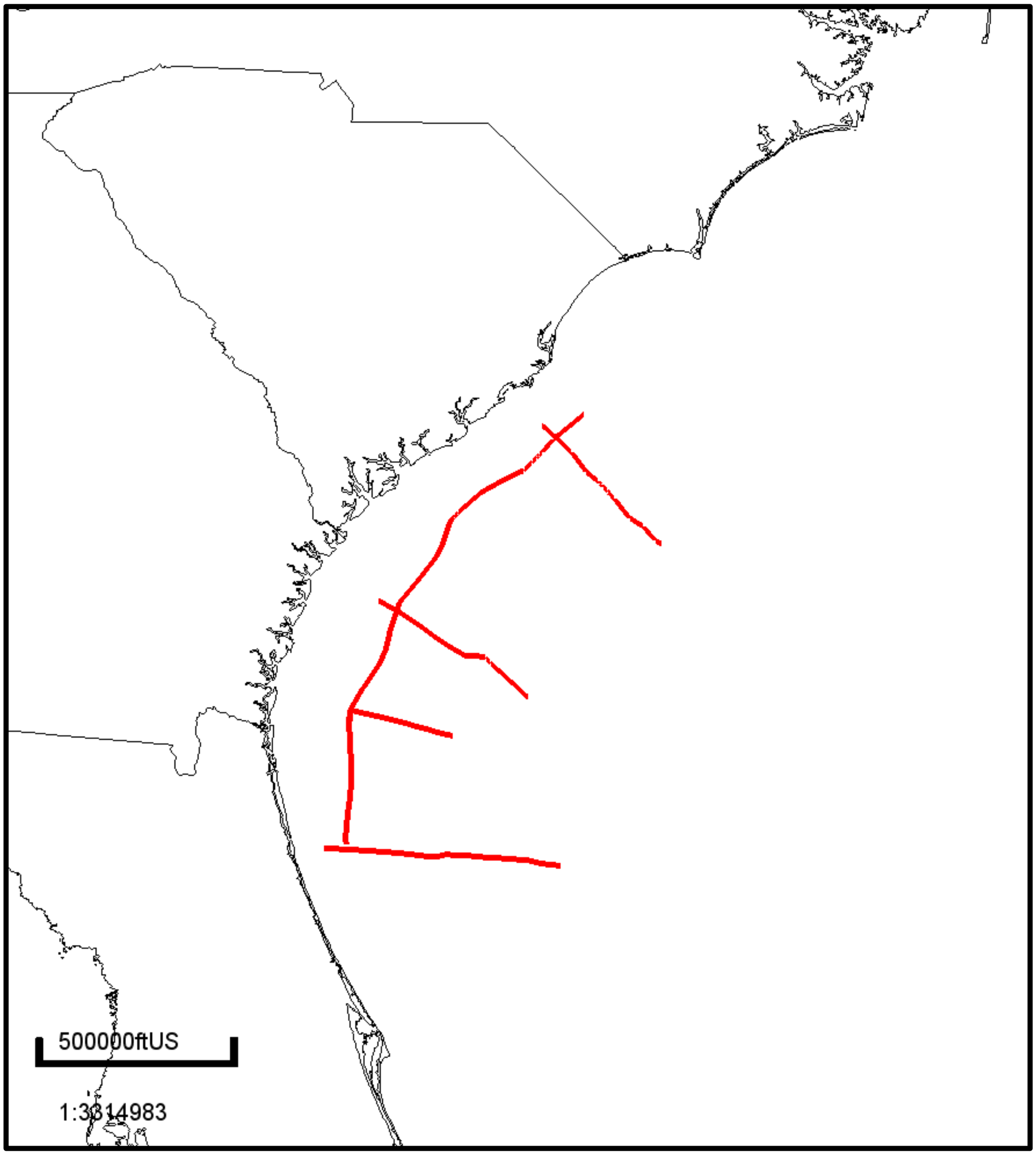

Figure 4.7: Pre-stack seismic reflection line locations

Table 4.2: Cruise IG1501 Seismic Data Acquisition Parameters	
Chief Scientist	Joel Watkins
Data Originating Institution	Institute for Geophysics, University of Texas at Austin
Beginning Date	5/9/1975
Ending Date	5/26/1975
Receiver Type	Hydrophone Streamer
Source Type	AirGun:Bolt4200
Survey Datum	WGS72
Source to Near Channel (meters)	267
Antenna to Source (meters)	undocumented
Number of Channels Recorded	24
Channel Length (meters)	91.4
Cable Receiver Depth (meters)	10
Source Volume (cubic inches)	4500
Source Pressure (bars)	24.1
Source Number	3
Source Depth (meters)	9

CHAPTER 5

HYPOTHESES

To satisfy the objective to "support industry's ability to predict CO_2 storage capacity in geologic formations to within ±30 percent," the seismic data must be converted to depth. This project will test a depth conversion workflow using a velocity model built in Schlumberger's *Petrel*. This model can be built by using previously published stacking velocity data from 2D seismic reflection surveys in the study area. A concentration of wells will provide some regional control off the coast of Georgia. For the remaining area, data points from published refraction studies will be employed as control. Hersey et al., 1959 provides data points for the tops of specific formations. Katz & Ewing, 1956 and Sheridan et al., 1966 provide points that lie somewhere within the specified formations. Additionally, pre-stack seismic data can be used as control. By performing velocity analysis, the extracted velocities can be compared with those already published from the 2D seismic lines in the area.

After quality control is performed on the velocity model, the seismic data can be depth converted. Main horizons, such as the Upper and Lower Cretaceous, will be depth converted. The stratigraphic depths of the horizons can be calculated by subtracting the depth converted seafloor horizon. Lastly, the formation surfaces will be filtered to be below the 2625 ft. threshold for supercritical CO_2 storage. Using this process, the overall area of formations that would create supercritical conditions for CO_2 will be known. The velocity model will allow this workflow to be replicated for any further seismic analyses. With the depth conversion complete, further rock properties analyses will need to be done to ultimately assess the feasibility of CO_2 sequestration in the study area.

CHAPTER 6

METHODOLOGY

With only 7 exploratory wells drilled in the South Atlantic Continental Margin, a lack of extensive well control exists in the study area. These wells are all located in a concentrated area off the coast of Georgia. As a result, there are no opportunities to tie seismic horizons to stratigraphic well tops outside of this concentrated area. Without these ties, the depths of stratigraphy in the seismic data are extremely difficult to estimate. Creating a broad 3D velocity model for time-depth conversion solves this problem. The depths of stratigraphic units found in the seismic refraction data serve as an alternative to well control. Even with the refraction data points acting as well control, there are still regions in the study area where interpolating surfaces would produce inaccurate results (Figure 6.1). 2D seismic reflection lines are located in these regions. The published stacking velocities along these seismic lines provide over 50,000 data points to create the velocity model. Thus, performing a time-depth conversion using data points from specific seismic reflection lines produce more accurate results than simply interpolating between well tops and refraction data points.

Using the published stacking velocities from seismic reflection data, a velocity model was created and quality controlled using *SeisSpace ProMAX, MATLAB, HampsonRussell* and Schlumberger's *Petrel Software* technology. This model provides a time-depth conversion for the study area. For quality control, well tops and seismic refraction data from 128 recording stations were employed when making the velocity model. After creation of the velocity model, major seismic horizons were depth converted. The horizons for the Upper and Lower Cretaceous, picked by Khaled Almutairi, were depth converted (Almutairi et al., 2017). Upper Jurassic and Paleozoic horizons, picked by Dawod Almayahi, were depth converted (Almayahi, 2018). The depths of these horizons were compared to the control points from well tops and seismic refraction data. The depths for the horizons were analyzed to identify areas that exceed the 2625 ft threshold for supercritical CO_2 storage. The velocity model was also used to depth convert the entire seismic dataset.

6.1 VELOCITY ANALYSIS

Semblance analysis is performed to measure the similarity of signals across a CDP gather. This indicates if specific velocities in an area are consistent between each trace. Semblance analysis is the sum of energy across traces over an interval of time normalized to the sum of energies in each trace (Figure 6.2, Equation 1, Yilmaz, 2011). In this equation, the semblance coefficient (S_c) is calculated for f_{ij}, the j^{th} sample of the i^{th} trace, using M number of channels for the window width N centered at k.

$$S_c(k) = \frac{\sum_{j=k-N/2}^{k+N/2}\left(\sum_{i=1}^{M} f_{ij}\right)^2}{\sum_{j=k-N/2}^{k+N/2}\sum_{i=1}^{M} f_{ij}^2} \quad (1)$$

Semblance analysis was performed in *MATLAB*. Stacking velocities were picked through the semblance analysis. The semblance contour map indicates the strength of correlation between several traces. Strong semblance points are picked on the cross section and the corresponding stacking velocities are recorded (Figure 6.3). These stacking velocities are converted to interval velocity using Dix equation (equation 2; Dix, 1955). In *Petrel*, the Dix conversion tool was used to convert the velocities. The interval velocity (v_{int}) is calculated using the stacking velocity from the n^{th} and ($n-1$) reflectors (Figure 6.4). The two-way-time (t_n) to each reflector is also used in the Dix equation (Dix, 1955).

$$v_{int} = \sqrt{\frac{v_n^2 t_n - v_{n-1}^2 t_{n-1}}{t_n - t_{n-1}}} \tag{2}$$

To create a velocity model, interval velocities must be calculated. This process begins with performing velocity analyses on selected pre-stack common midpoint gathers. Specifically, comparing extracted velocities from velocity analysis to nearby stacking velocity points from the seismic data adds control to the velocity model. The majority of the velocity analyses focus on areas near those stacking velocity points. In total, velocity analysis was performed on 247 CDP gathers in the study area. While a minority of these CDPs contained inadequate traces for semblance analysis, velocity data from over 200 CDPs was imported to *Petrel* (Figure 6.5). The CDPs with inadequate traces most likely contained multiples that created error in the semblance analysis.

Using the interval velocities, the depths of each layer can be calculated in feet using the picked two-way-time depth from the stacked seismic reflection data (Figure 6.6). With the depths of stratigraphic units in feet, the storage capacity of potential reservoirs can be estimated. Knowledge of the depths and thicknesses of reservoirs is a major step in the process to drill and store CO_2 in the Southeastern United States Atlantic Continental Margin.

6.2 MODEL INPUTS

Stacking velocity data points were found in .geo files for several 2D seismic surveys performed by BOEM. With code from our SOSRA colleague Charles Schlosser at Virginia Polytechnic Institute and State University, over 50,000 stacking velocity data points were extracted from the seismic surveys. These stacking velocities were extracted during the original processing for the surveys. Surveys in which the stacking velocities were extracted are B-01-81-AT, B-02-80-AT, B-05-81-AT, B-09-75-AT, B-16-76-AT, B-17-77-AT, B-28-75-AT, and B-29-76-AT (Figure 6.7). The stacking velocities were imported into *Petrel* and Dix conversion was used to convert the stacking velocities to interval velocities.

Additionally, several seismic surveys have stacking velocities listed in the .pdf files associated with the seismic lines (Figure 6.8). Given the distribution of the data points from the .geo files, inputting data points from the .pdf files for surveys E02-77 and E28-75 were most beneficial to the model. Over 5,000 data points were manually inputted into Microsoft Excel for import into *Petrel* for the velocity model. These points help fill in gaps in the Blake Plateau that were not covered by the .geo files. However, there are illegible .pdfs. If given the time to analyze, these .pdfs could provide additional data points to cover the extent of the Blake Plateau.

In all, approximately 54,000 data points for interval velocity were used to create the velocity model (Figure 6.9). A velocity cube encompassing the data points in the study area was constructed in *Petrel* (Figure 6.10). Interpolating the interval velocity data points created this cube. This cube was used to create a simple velocity model to depth convert seismic horizons and the seismic data. However, there were several erroneous data points that created dramatic changes in the velocity model. These data points were either caused by human input error from the .pdf files or processing errors for the published stacking velocity data.

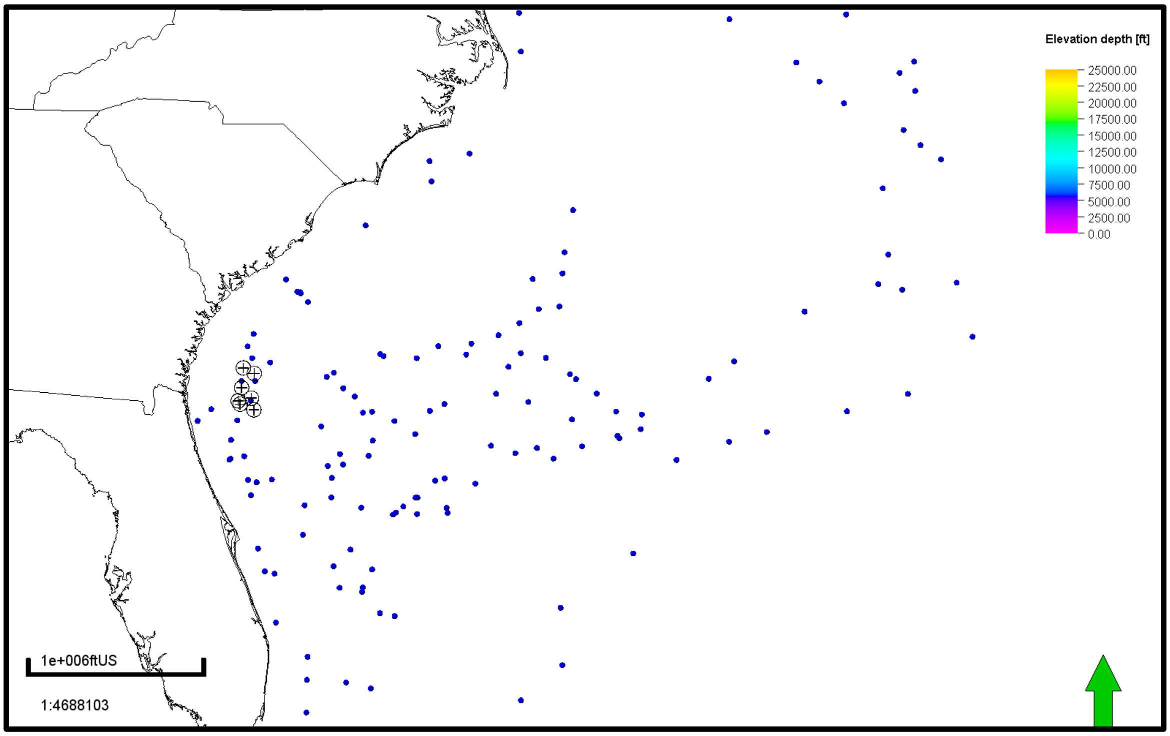

Figure 6.1: Distribution of refraction data points (blue) and wells (black crosshairs). Effective interpolation requires additional data between existing points.

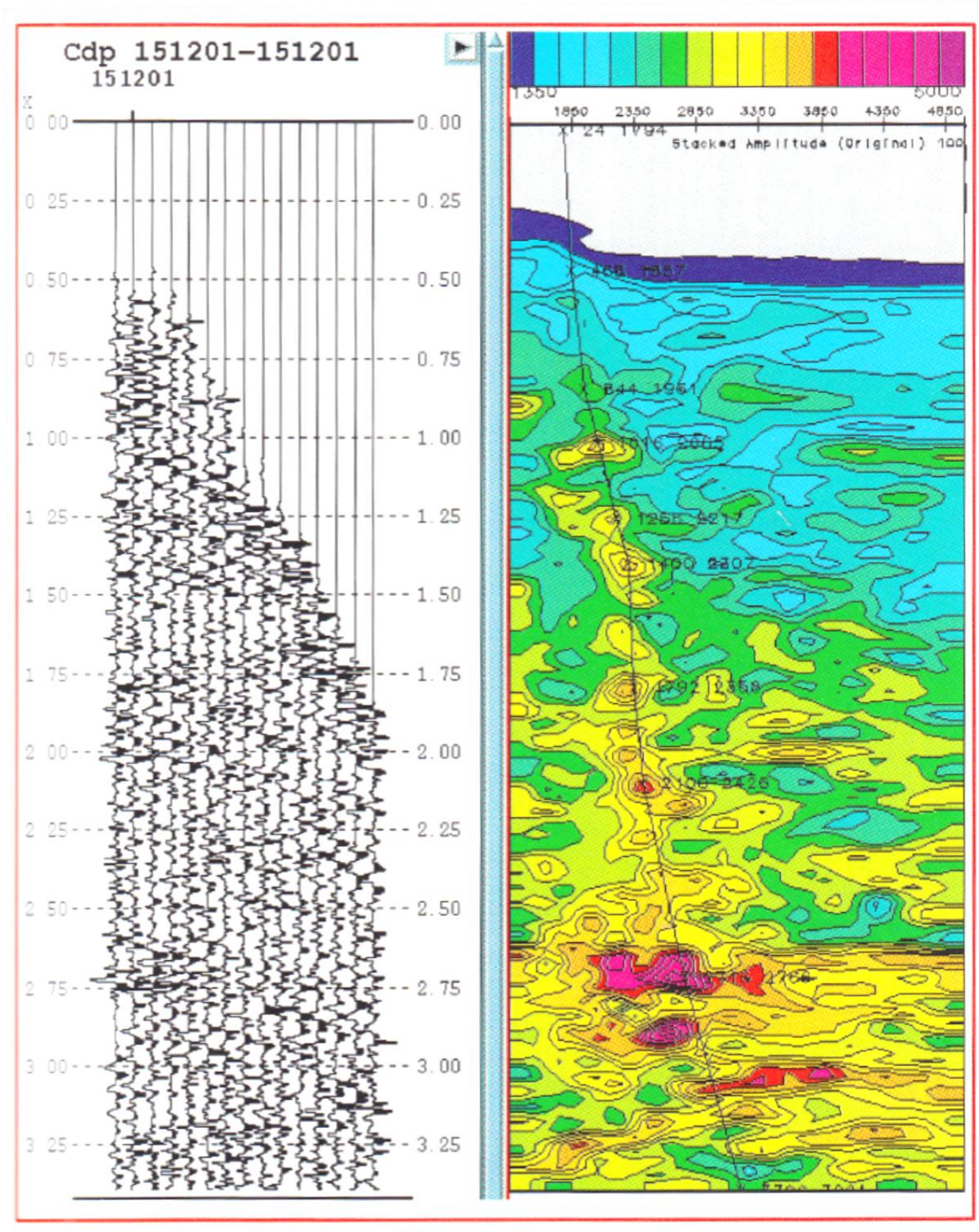

Figure 6.2: Textbook example of semblance analysis on a CDP gather. Semblance coefficient is illustrated in the contour map. Velocities are picked at points of high semblance. (Yilmaz, 2001)

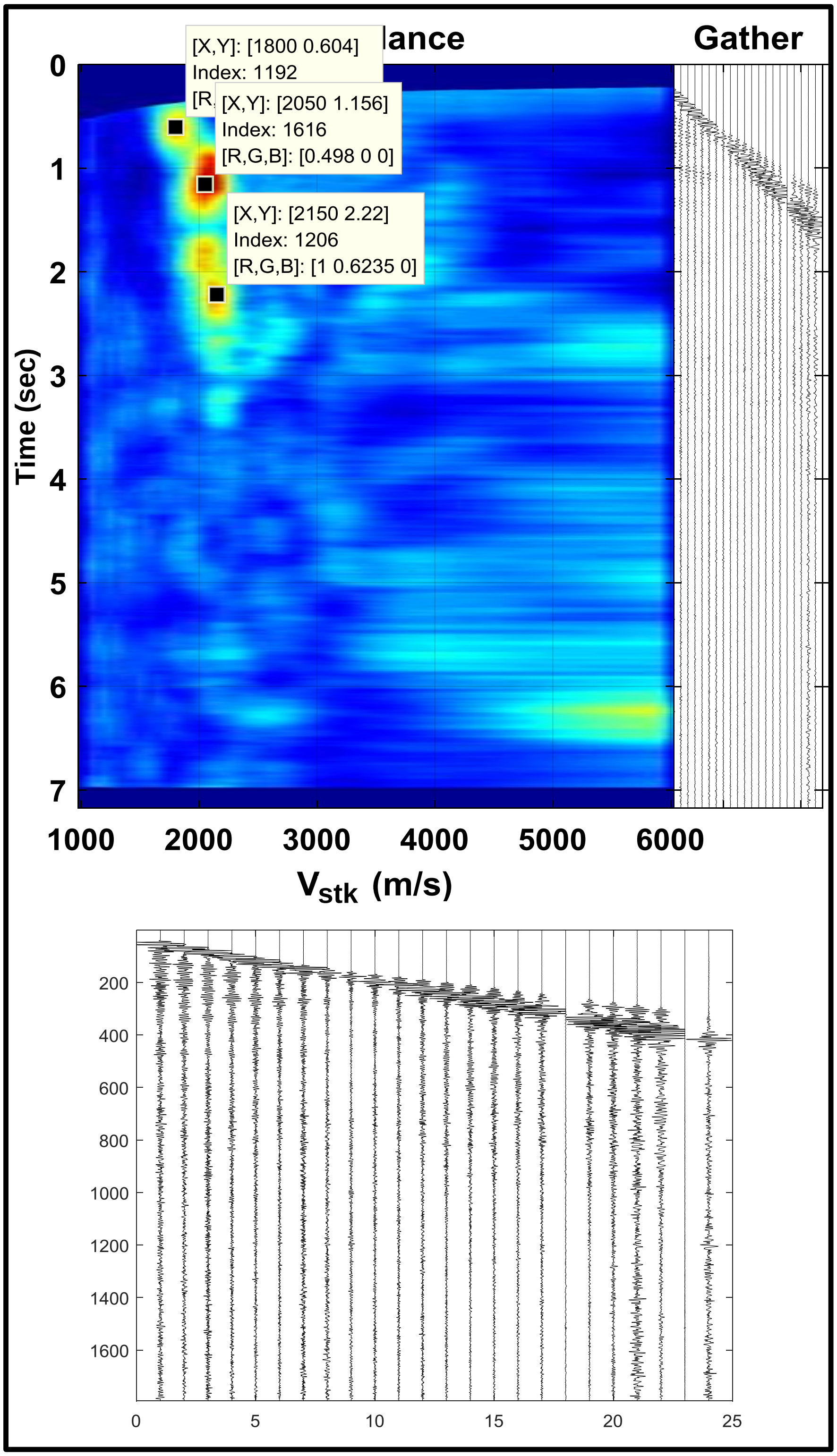

Figure 6.3: Velocity analysis for traces 7001-7024 on line se-3-28. Above: semblance with stacking velocity picks. Semblance code provided by CREWES Project; Below: CDP gather

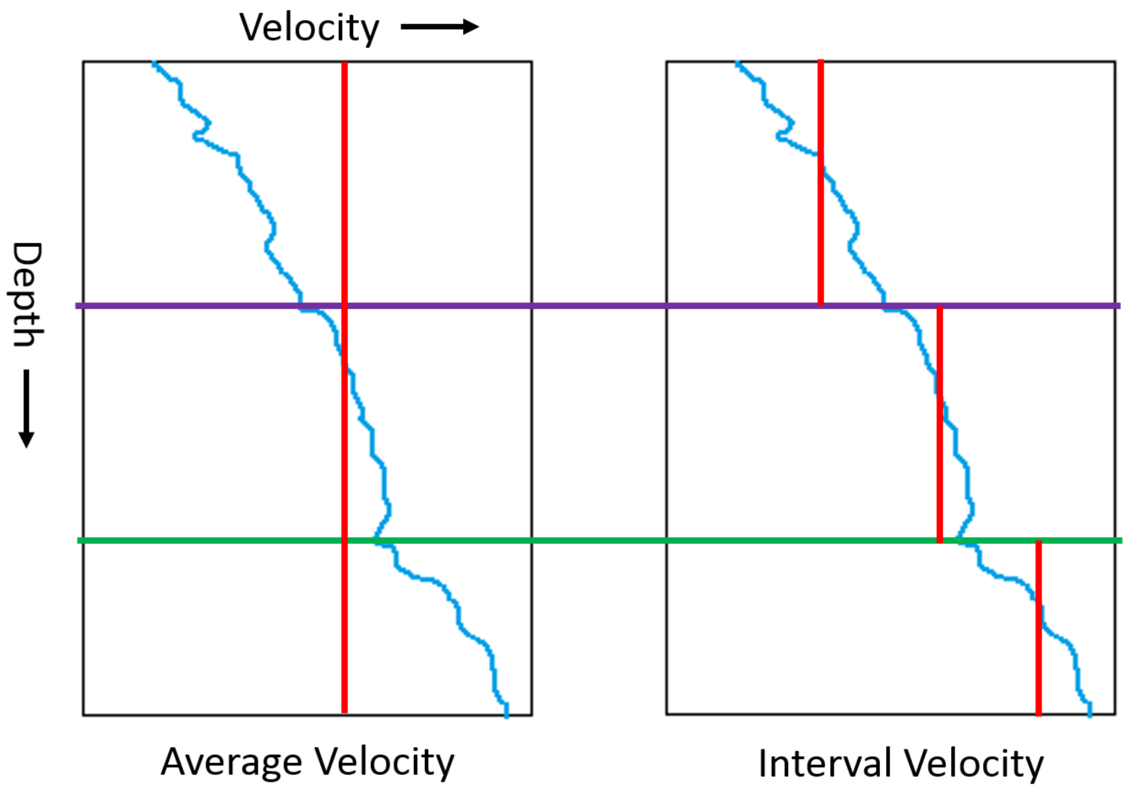

Figure 6.4: Conversion of average velocity to interval velocities for 3 stratigraphic units.

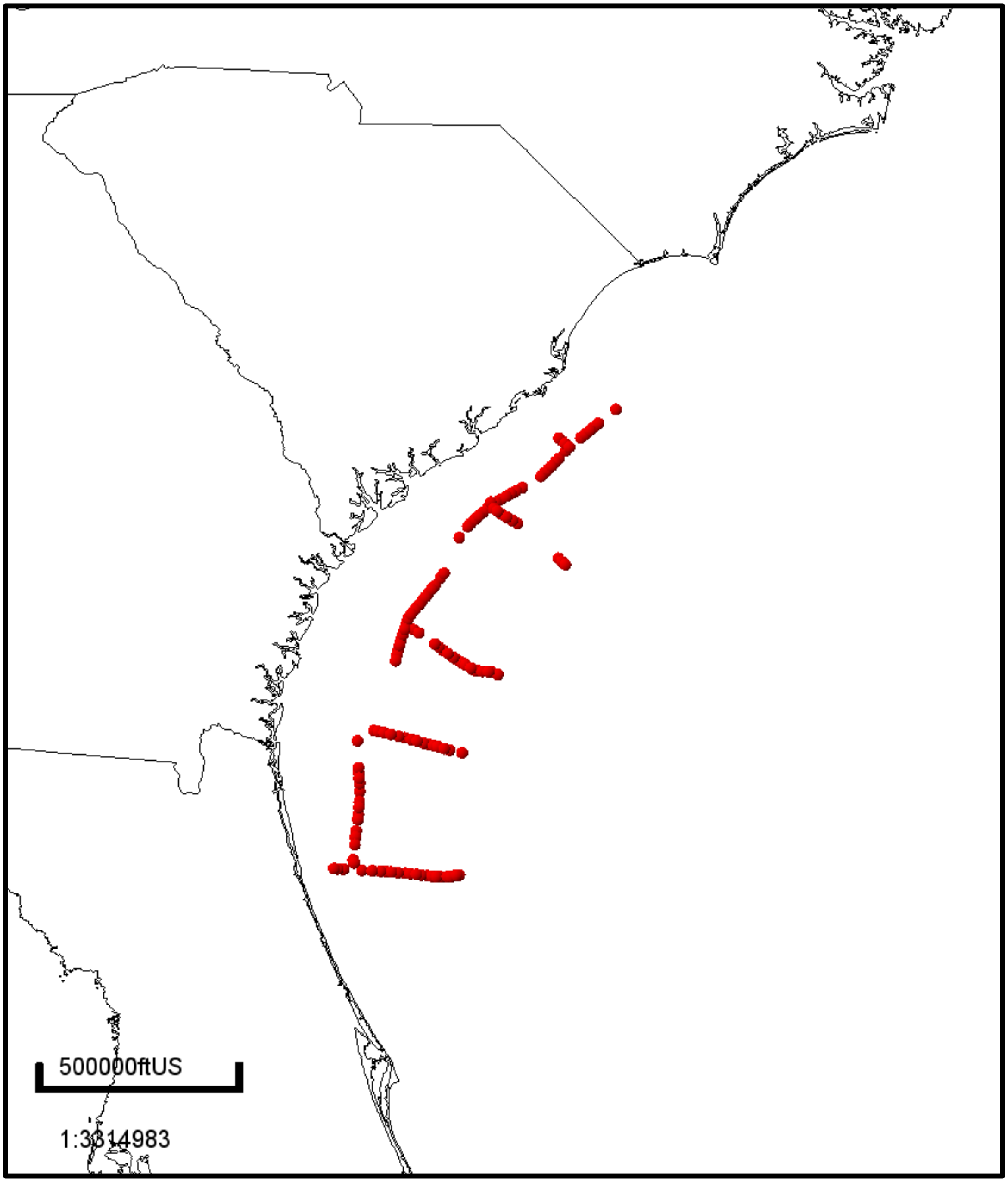

Figure 6.5: Locations of extracted stacking velocities data points from velocity analyses

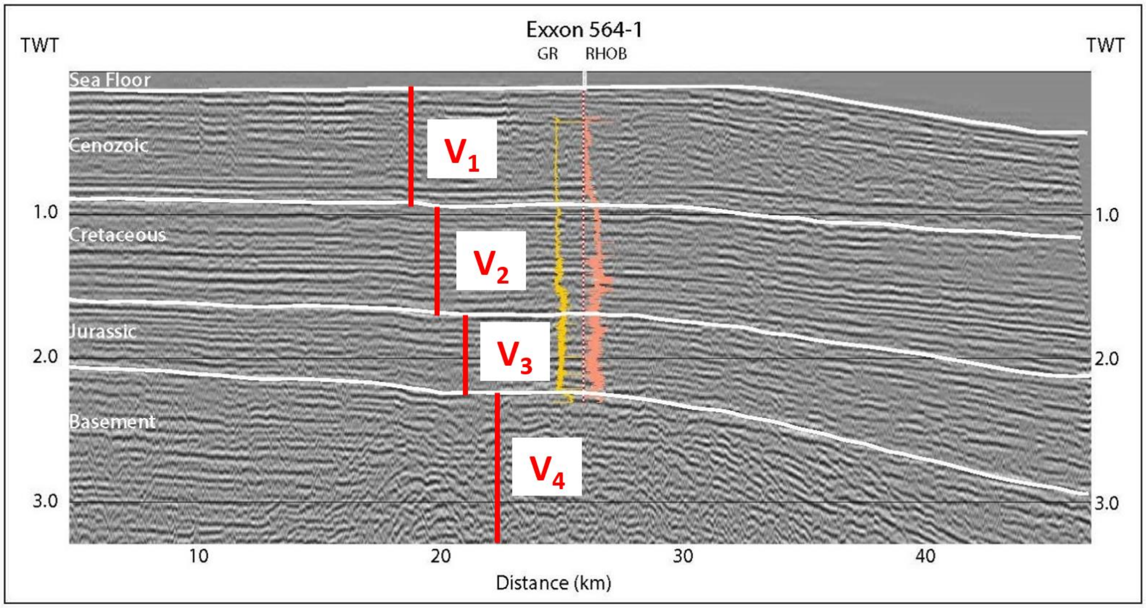

Figure 6.6: Interval velocities overlain on a 2D seismic line with seismic horizons picked in two-way-time. Depths in feet can be calculated using the interval velocities and two-way-time depths

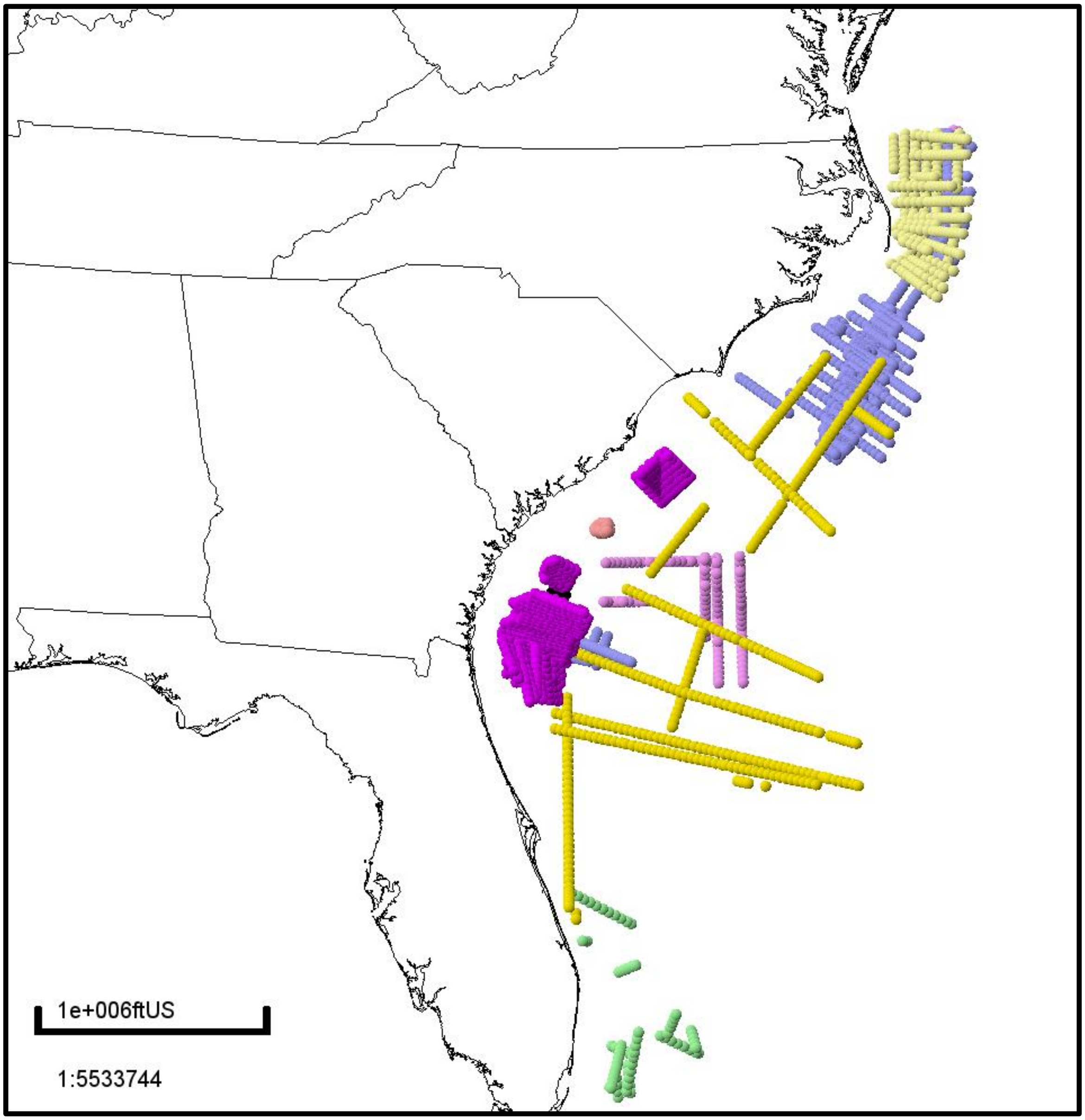

Figure 6.7: Locations of stacking velocity data points from .geo files. Green: B-05-81; Black: B-29-76; Magenta: B-09-75; Gold: B-28-75; Purple: B-02-80; Pink: B-01-81; Light yellow: B-16-76; Light pink: B-17-77

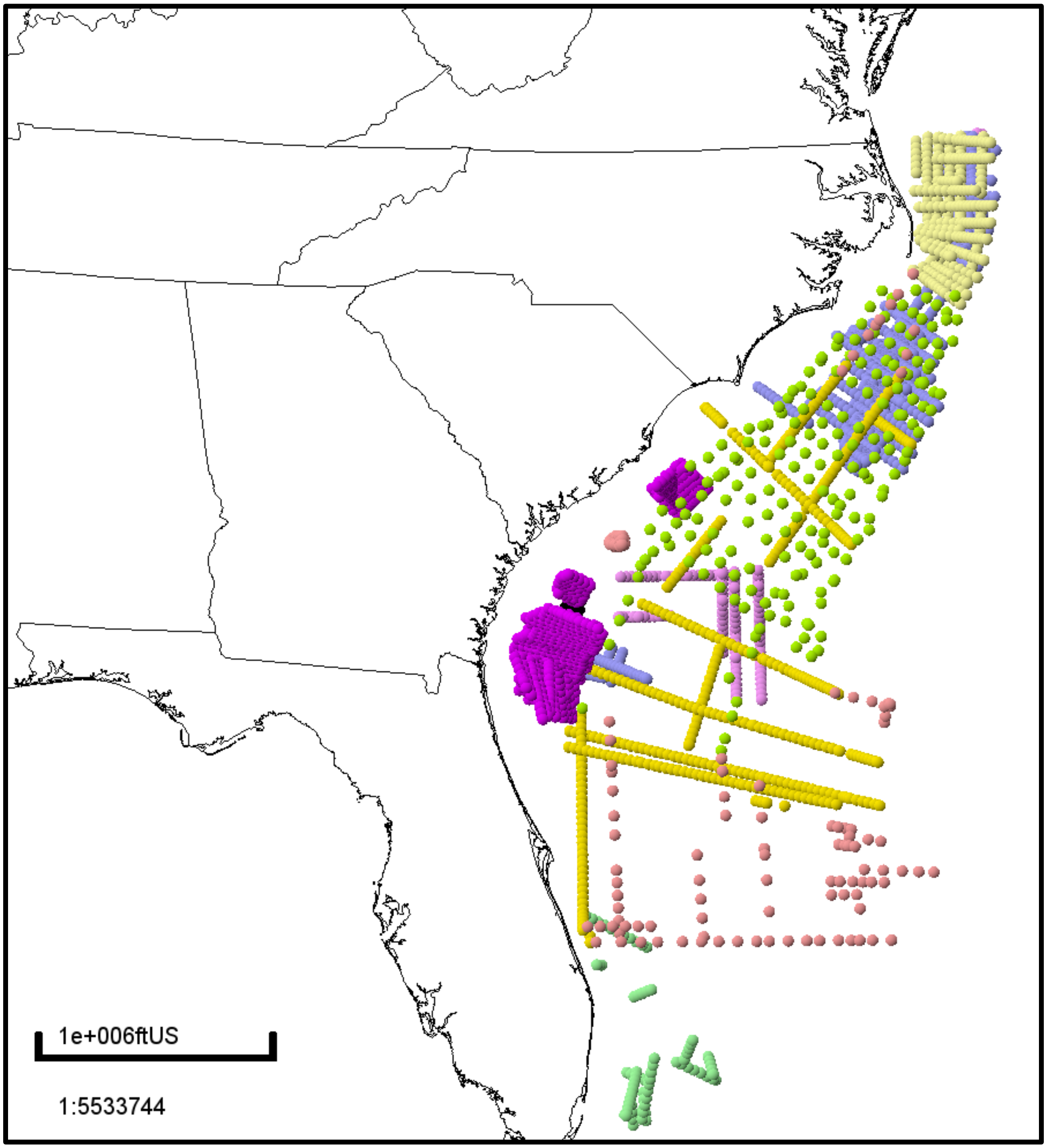

Figure 6.8: Stacking velocity points from .pdf files added; Green: E02-77; Light pink: E28-75

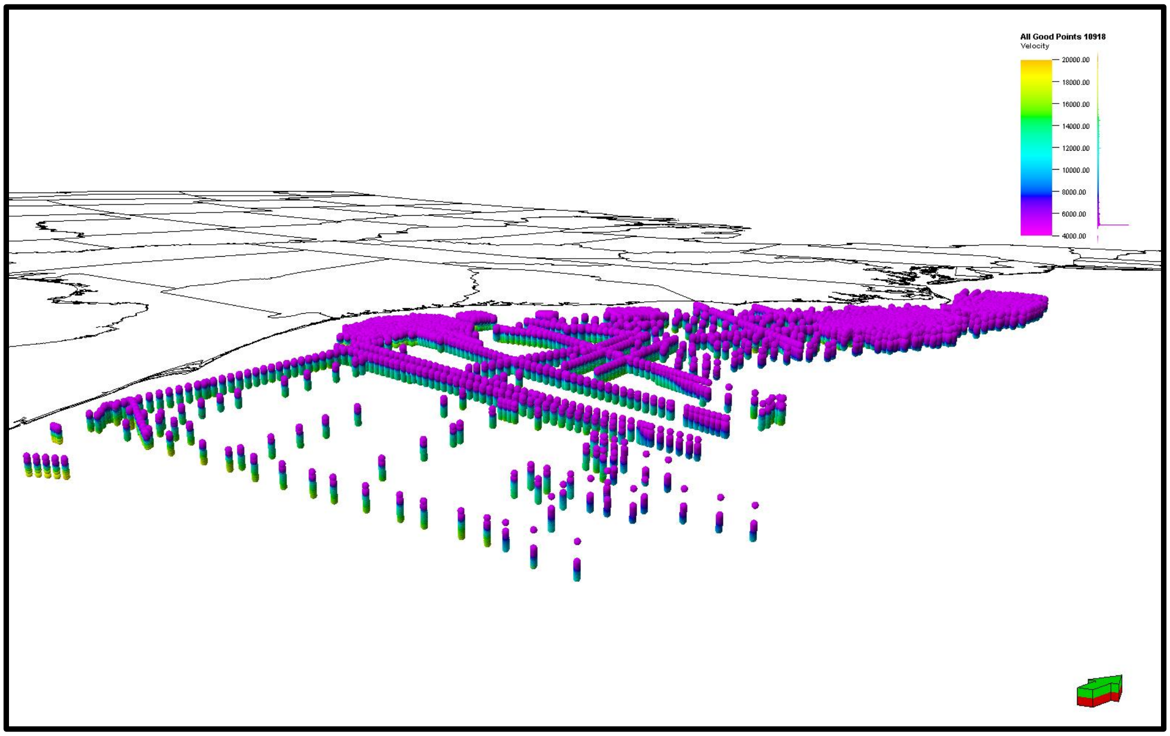

Figure 6.9: 3D view of all stacking velocity points with velocity color coding

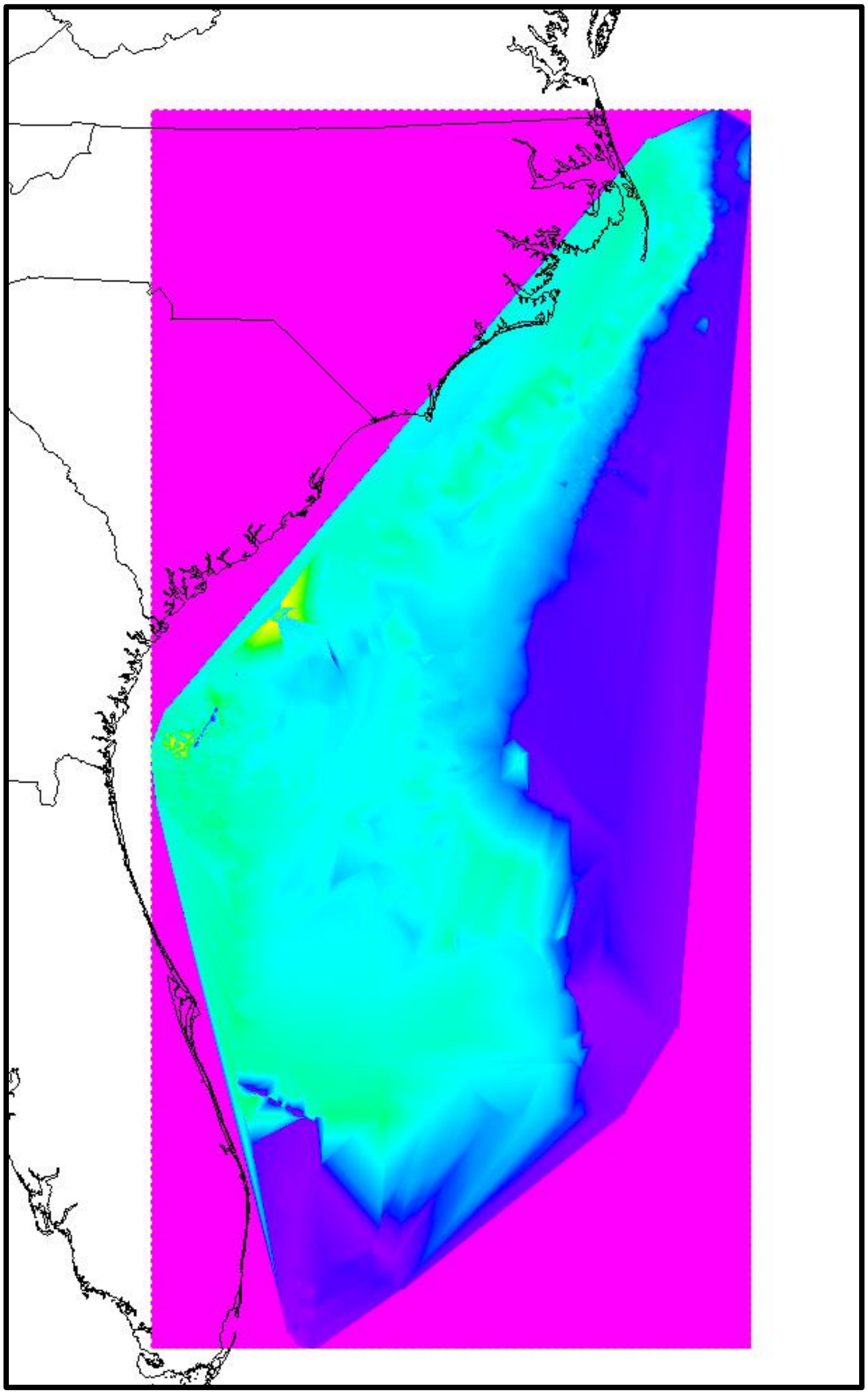

Figure 6.10: Initial interval velocity cube; time slice at 2 sec TWT

CHAPTER 7

DISCUSSION

There were several erroneous data points that created dramatic changes in the velocity model. These data points were either caused by human input error from the .pdf files or processing errors for the published stacking velocity data. Some data point errors, such as an entire seismic line causing a bust in the velocity model, were easy to spot and fix (Figure 7.1). It was discovered that all the published stacking velocity data for seismic survey B-29-76-AT was much higher than all other data surrounding it (Figure 7.2) This situation occurred in 2 areas along the southeast Georgia Embayment. Stacking velocities extracted from velocity analysis on nearby seismic lines proved to be much closer to data from survey B-17-77-AT (Figure 7.3, Table 7.1). As a result of this analysis, seismic survey B-29-76-AT was removed from the velocity model altogether.

Several iterations of the velocity cube and velocity model were created and refined throughout the project. Just one bad data point can create a bust in the velocity model, drastically altering the seismic data and horizons after depth conversion. After removing these troublesome data points, the final velocity cube and velocity model was created (Figure 7.4). Domain conversion from time to depth was carried out for seismic horizons and the 2D seismic lines in the study area (Figures 7.5 & 7.6).

There is no smoothing operator for velocity cubes in *Petrel*. As a result, surfaces were smoothed after the depth conversion to create surfaces that more accurately reflect the geology. The surfaces were smoothed with 2 iterations and a filter width of 5 to remove these spikes.

For control on the accuracy of the velocity model, refraction data points marking the top of formations such as the Upper Cretaceous intended to be used from a study by Hersey et al., 1959. However, after creating the model it was apparent that several data points marking the Upper Cretaceous were, in some cases, over 2,000 ft higher than the Upper Cretaceous seismic horizon. To resolve this issue, the USGS study published on the COST GE-1 well was referenced. In the stratigraphic column derived from the COST GE-1 well logs and core, the top of the Upper Cretaceous begins at 3535 ft TVD (Scholle, 1979). Conversely, a data point from Hersey et al., 1959 located 3 miles from the COST GE-1 well has a depth of 260 ft for the top of the Upper Cretaceous. The depth-converted top of Upper Cretaceous horizon yields a 3467 ft depth at the area of the COST GE-1 well. There is a 68 ft difference in the depths between the Upper Cretaceous horizon and the COST-GE 1 Upper Cretaceous formation top (Figure 7.7). As a result, it can be confidently stated that for the region around the COST GE-1 well, the velocity model more accurately reflects the geology than that published in Hersey et al., 1959.

With the loss of data points from Hersey at al., 1959 as control, there remains a lack of control on the velocity model. For the other two refraction studies, Katz & Ewing 1956 and Sheridan et al., 1966, the tops of formations are not published. Instead, these studies publish points at various depths and are labeled as being within a certain formation. At the COST GE-1 well, the Upper Cretaceous and Lower Cretaceous have thicknesses of 2,500 ft and 3,500 ft respectively (Figure 7.8). Therefore, these 2 studies provide minimal control, as they do not indicate where the points lie within each formation.

With the 3 refraction studies providing minimal control, the 7 wells drilled in a concentrated area off the coast of Georgia serve as the only control for the area. The velocity data from these wells were not included in the velocity model. Instead, the wells were used to compare against the velocity model. As previously stated, at the COST GE-1 well, the Upper Cretaceous formation top is at 3535 ft. compared to 3467 ft. in the velocity model. The difference of 68 ft. between the velocity model and well data provides confidence in the accuracy of the velocity model. The top of the Lower Cretaceous depth converted surface is 5278 ft. at the COST GE-1 well. This varies from the approximately 5950 ft. depth from the USGS report (Scholle, 1979). This may be the result of an initial poor well tie during the seismic horizon picking process. The depth converted Paleozoic surface has a depth of 11183 ft. at the COST GE-1 well. The USGS report for the COST GE-1 well published a depth of approximately 11050 ft. for the Paleozoic (Scholle, 1979). This difference of less than 150 ft. between the model and the actual depth further increases confidence in the velocity model.

Determining if formations are deeper than 2625 ft. for supercritical storage is vital to complete the objective to "support industry's ability to predict CO_2 storage capacity in geologic formations to within ±30 percent." For the Upper Cretaceous, a surface created from the horizon picked in two-way-time by Khaled Almutairi was depth converted (Almutairi et al., 2017; Figure 7.9). The seafloor horizon was picked for this project in order to estimate the stratigraphic depths of formations. The seafloor horizon was domain converted (Figure 7.10). The datum for the seismic data was the sea level. Thus, subtracting the depth of the seafloor from the Upper Cretaceous provides the stratigraphic depth of the Upper Cretaceous (Figure 7.11). The new stratigraphic depth surface for the Upper Cretaceous was filtered to eliminate any area with depths less than 2625 ft. In terms of depth, portions of the Upper Cretaceous are suitable for CO_2 storage. The total surface area for the picked Upper Cretaceous in the study area is 94,173 mi^2. When considering the necessary 2625 ft. depth for supercritical storage, the potential storage area for the Upper Cretaceous shrinks to 58,609 mi^2 (Figure 7.12). Overall, 62% of the top of the Upper Cretaceous would be suitable for CO_2 to undergo the phase change from gas to a supercritical fluid. Several further investigations on potential reservoirs and seals are needed to further constrain the possibility of CO_2 sequestration in the study area.

The same process was followed for the top of the Lower Cretaceous horizon picked by Khaled Almutairi (Almutairi et al., 2017). The total area covered by the Lower Cretaceous horizon picks in the study area is 91,466 mi^2 (Figure 7.13). 84,108 mi^2 of the Lower Cretaceous lies below a stratigraphic depth of 2625 ft. (Figure 7.14). For 92% of the Lower Cretaceous formation top, CO_2 would be stored as a supercritical fluid.

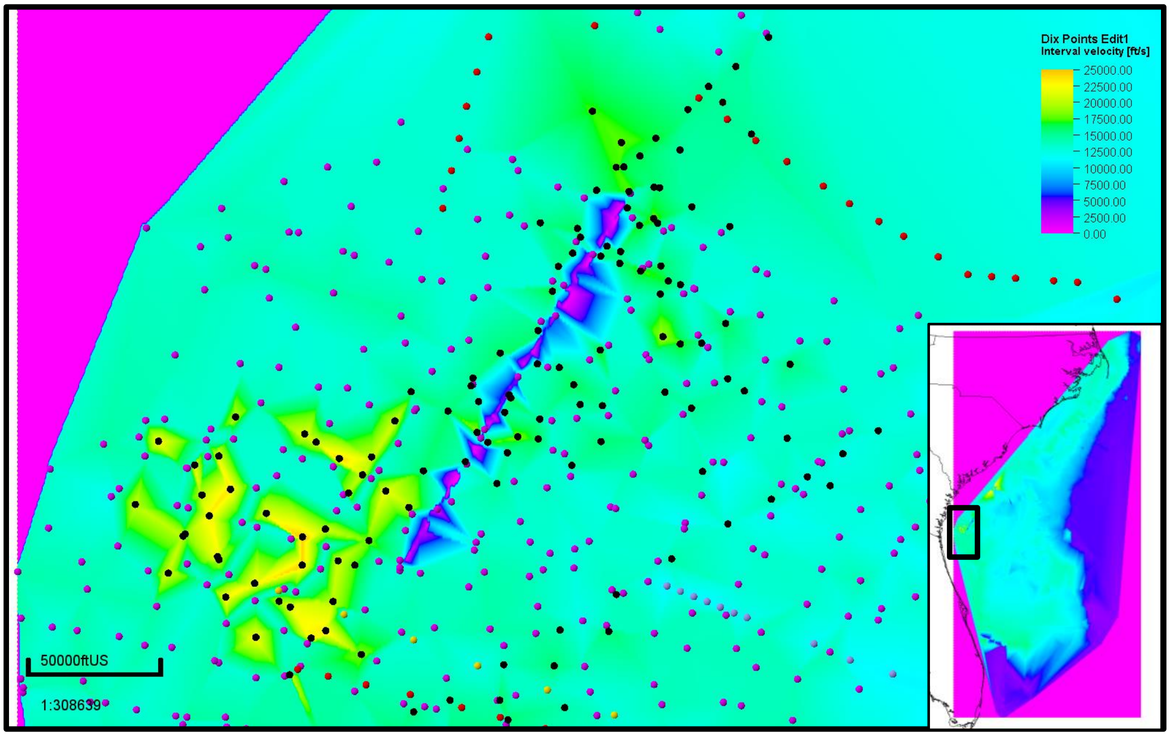

Figure 7.1: Example of data points creating anomalies in the velocity model. Time slice at 2 sec TWT

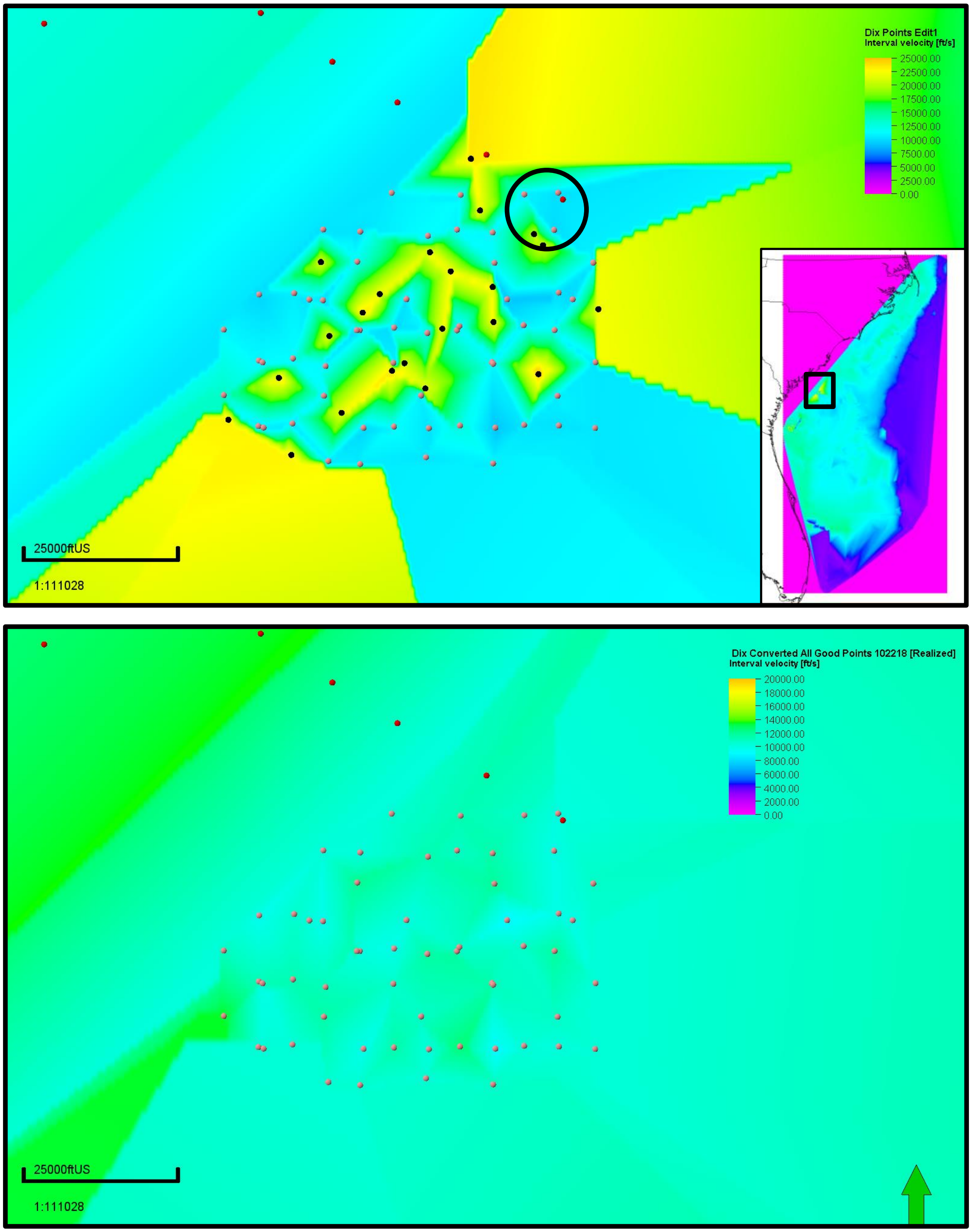

Figure 7.2: Above: Survey B-29-76 (black) creating anomalies in the velocity model compared to B-17-77 (light pink). Red point in black circle: CDP #281 on line se-3-28 for velocity comparison to adjacent points. Below: velocity model with B-29-76 removed

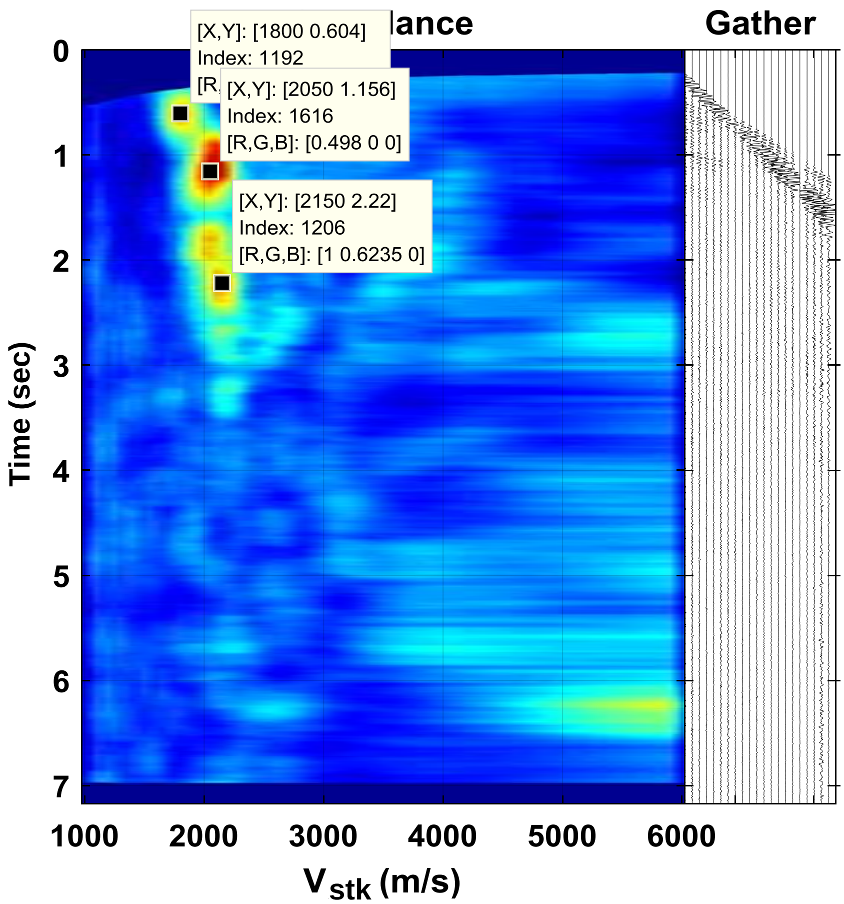

Figure 7.3: Velocity analysis on CDP gather 281 for line se-3-28. Semblance code provided by CREWES Project

Table 7.1: Stacking Velocity Analysis Comparison					
CDP 281		B-17-77		B-29-76	
Time (ms)	Velocity (ft/sec)	Time (ms)	Velocity (ft/sec)	Time (ms)	Velocity (ft/sec)
604	5906	0	4800	0	5000
1128	6723	150	4900	400	5880
2220	7061	750	6600	800	6663
		1000	7000	1200	7297
		1600	7800	2000	11300
		2700	9000	3000	17167
		6000	11500	4000	18722

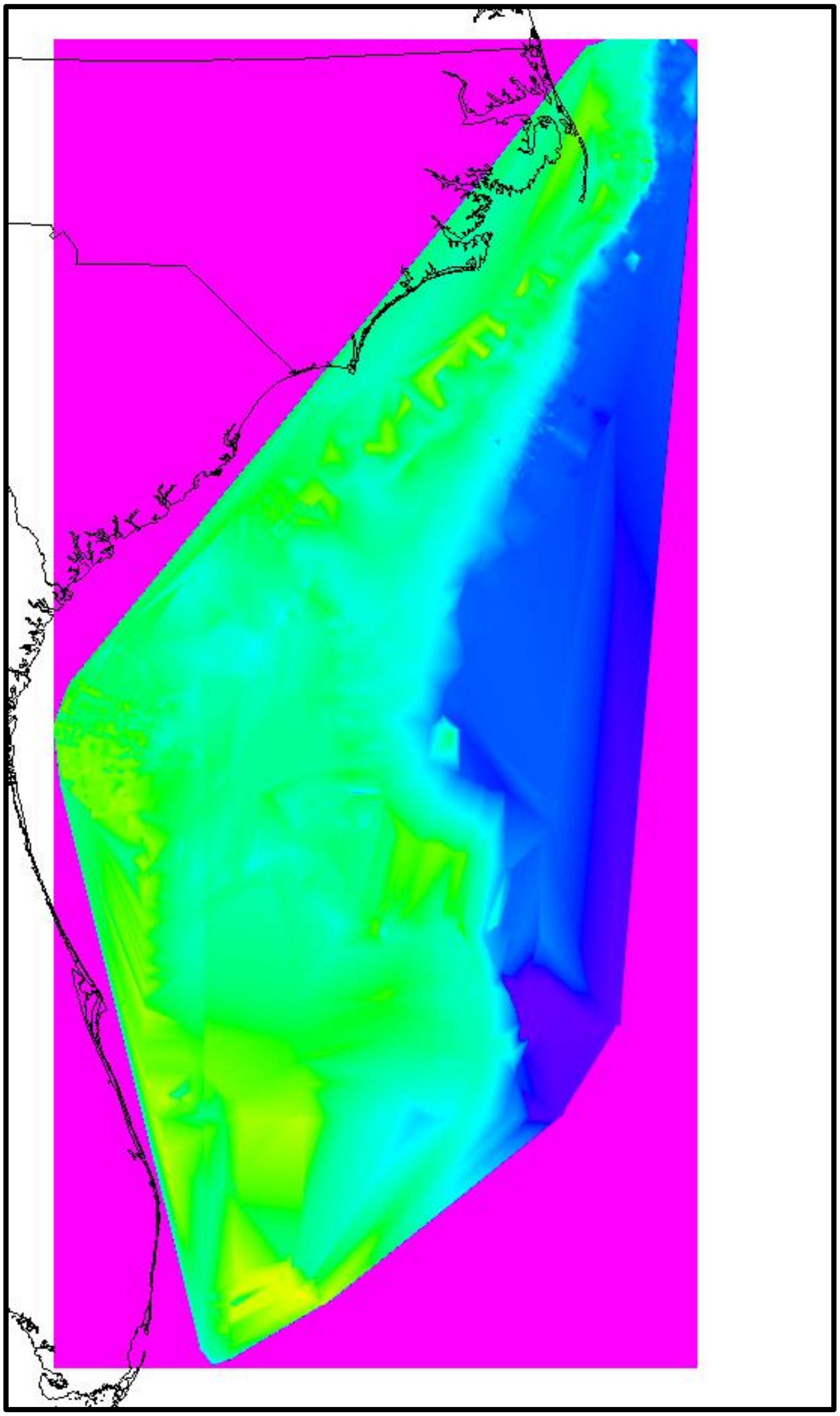

Figure 7.4: Final interval velocity cube; Time slice at 2 sec TWT

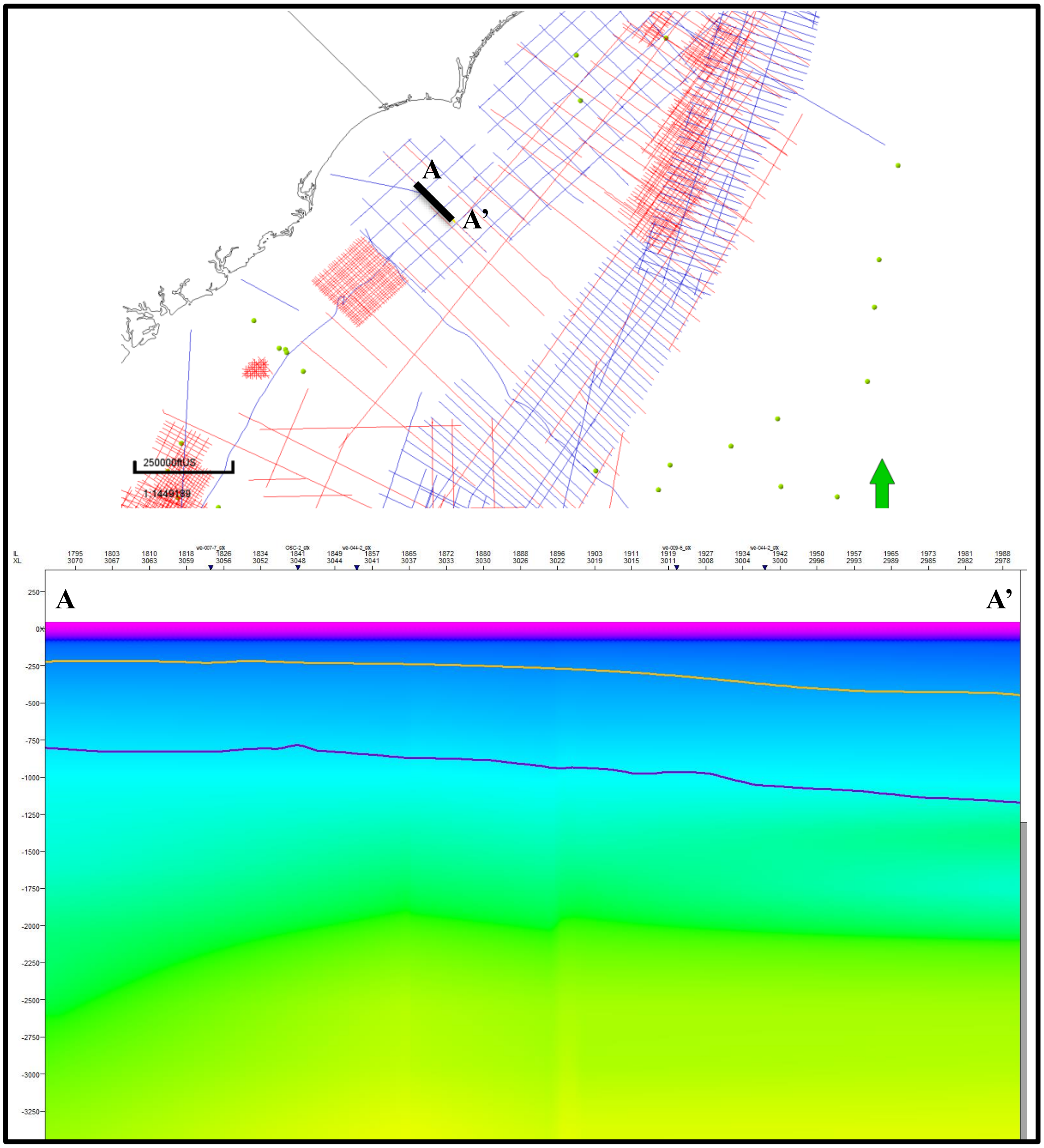

Figure 7.5: Velocity profile along 2D seismic line. Orange: top of Upper Cretaceous; Purple: top of Paleozoic

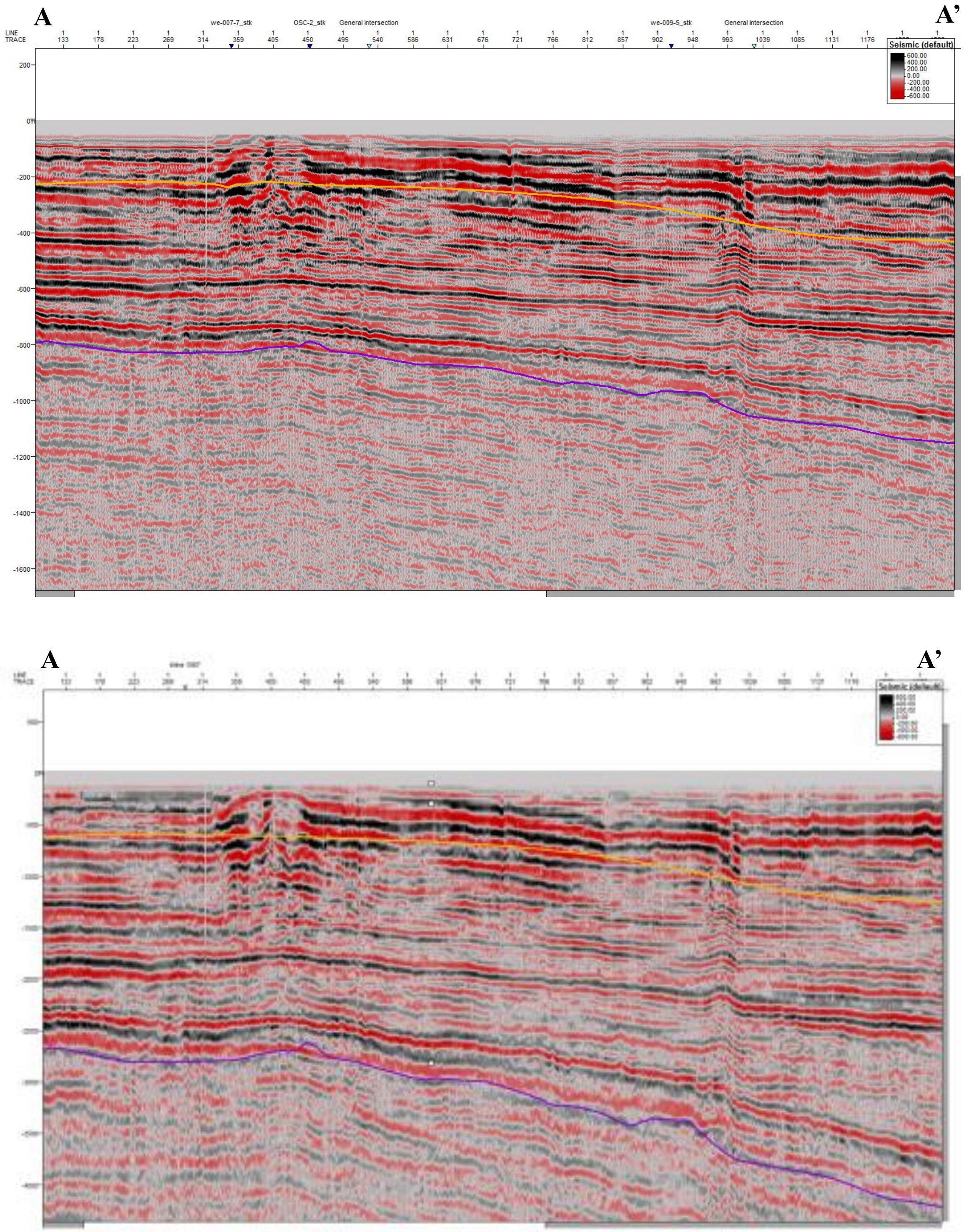

Figure 7.6: Depth converted seismic line at A-A’. Above: depth in sec TWT; Below: depth in feet

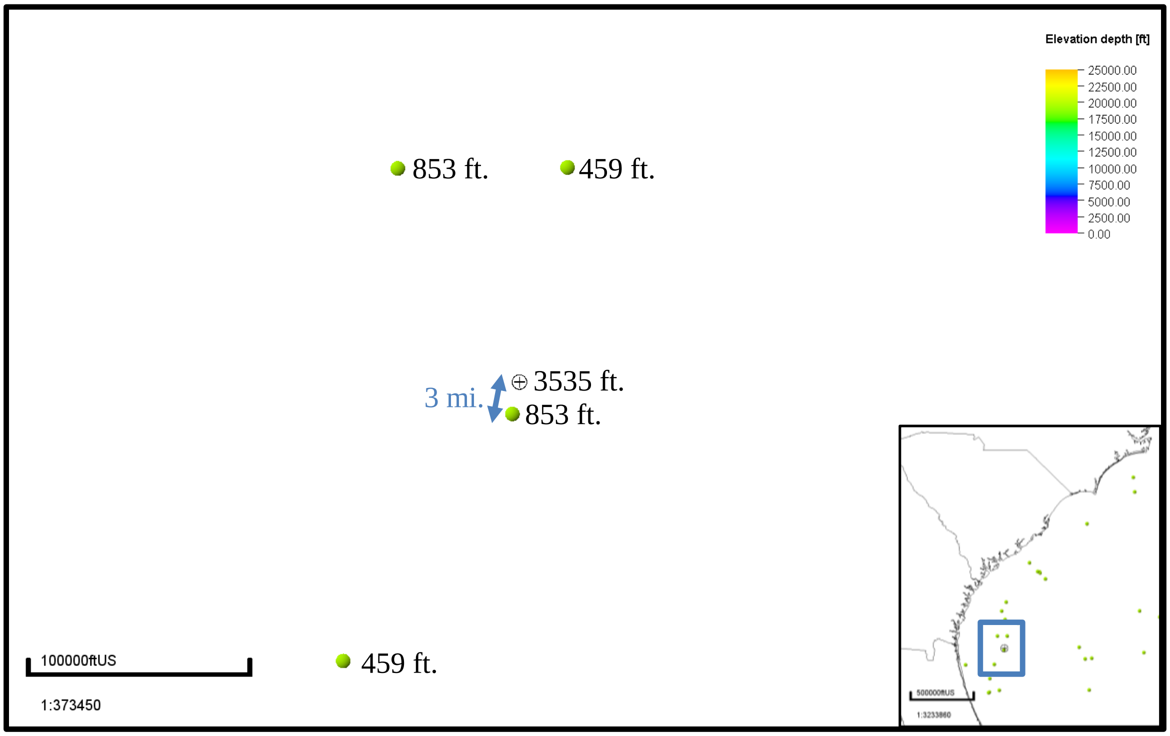

Figure 7.7: Top of Upper Cretaceous depths for COST GE-1 well (black crosshairs) and Hersey et al., 1959 (green dots).

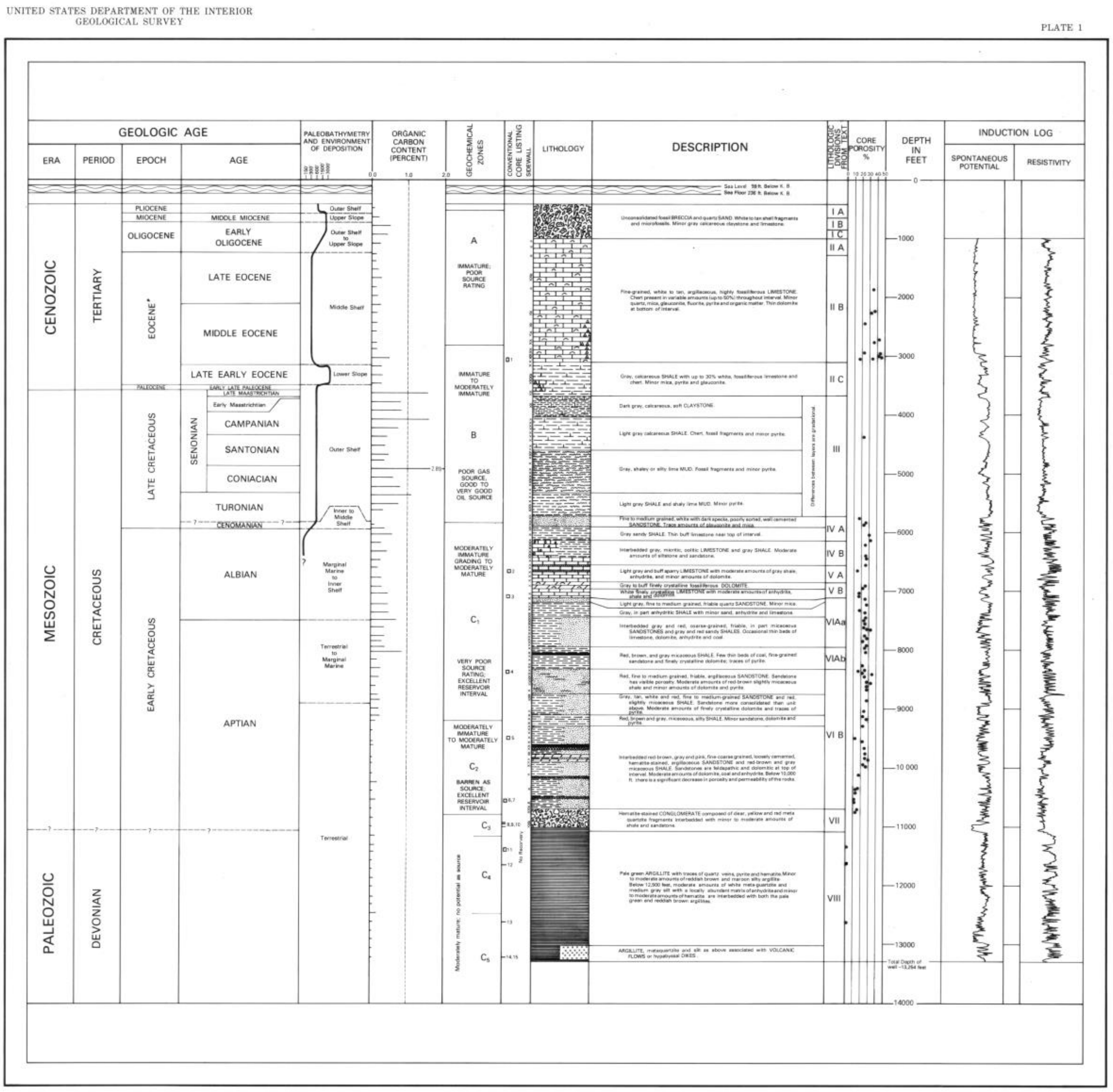

Figure 7.8: Stratigraphic column of COST GE-1 well (Scholle, 1979)

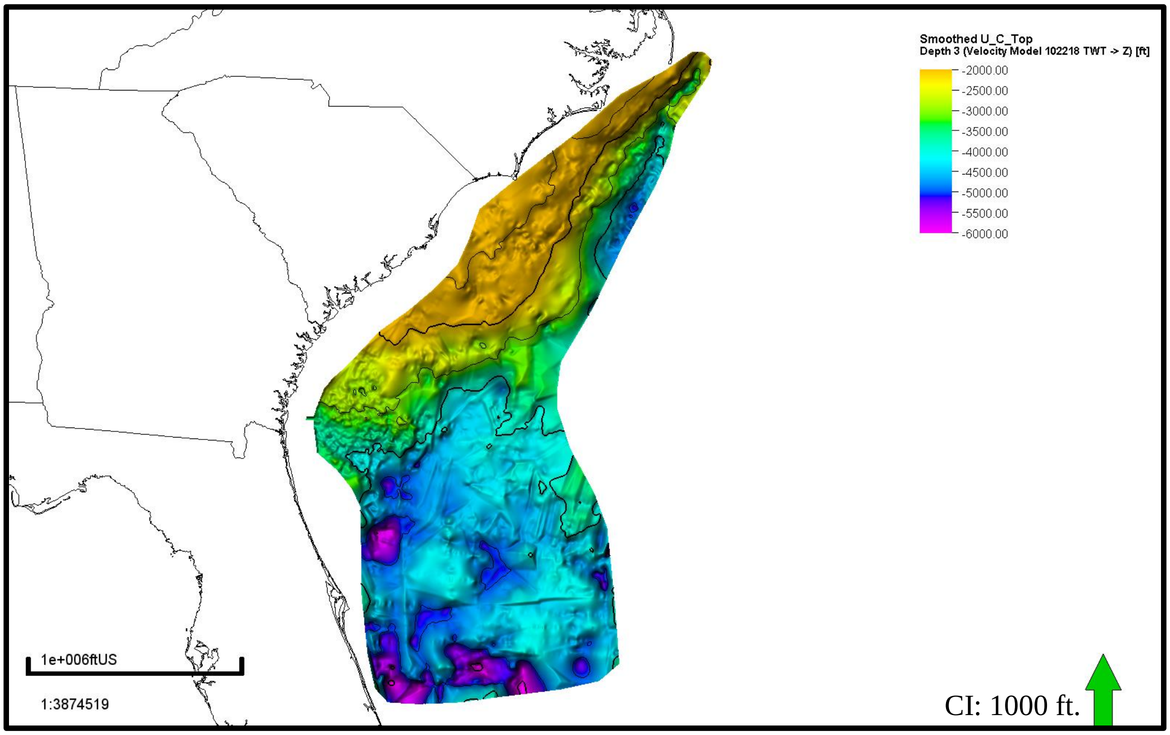

Figure 7.9: Upper Cretaceous surface from horizon picks

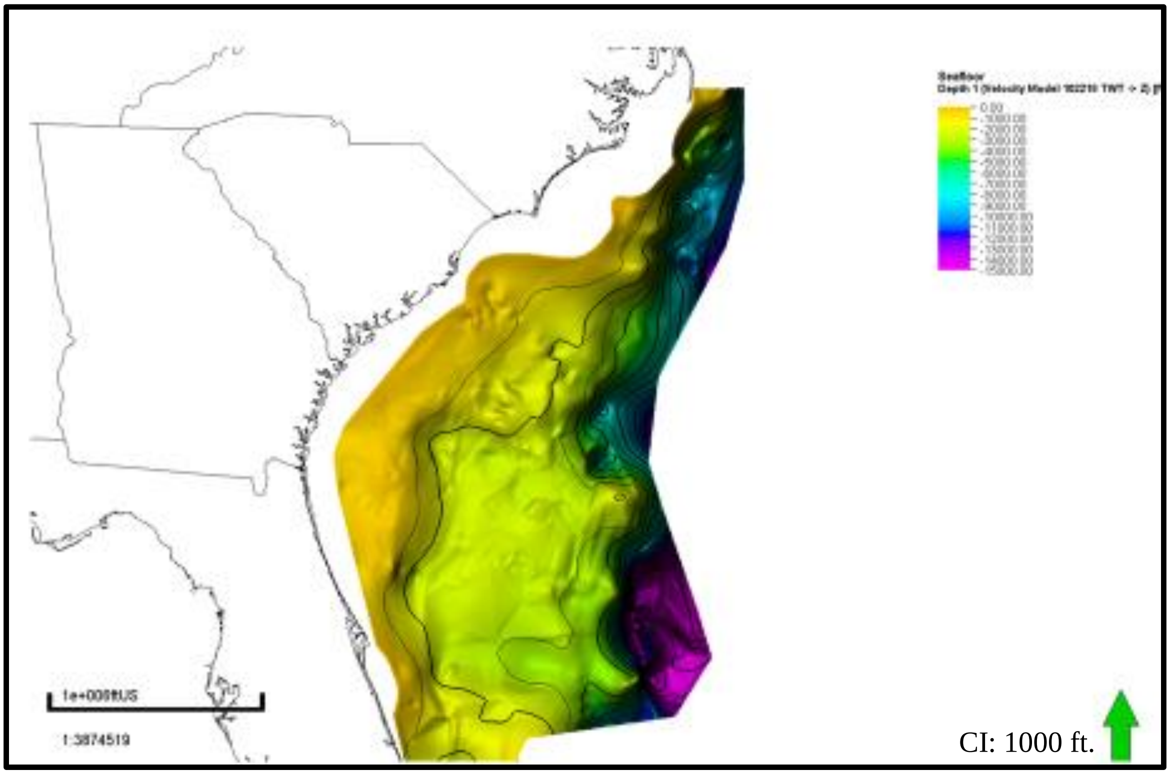

Figure 7.10: Seafloor surface from horizon picks

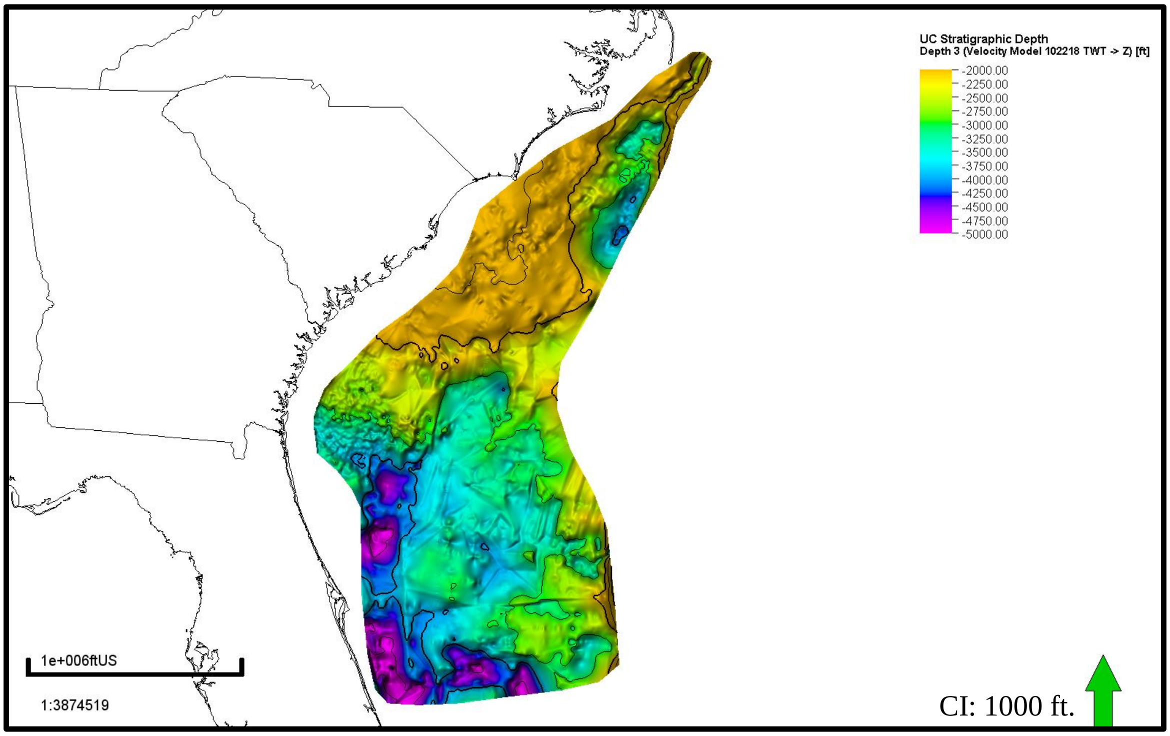

Figure 7.11: Upper Cretaceous stratigraphic depth surface

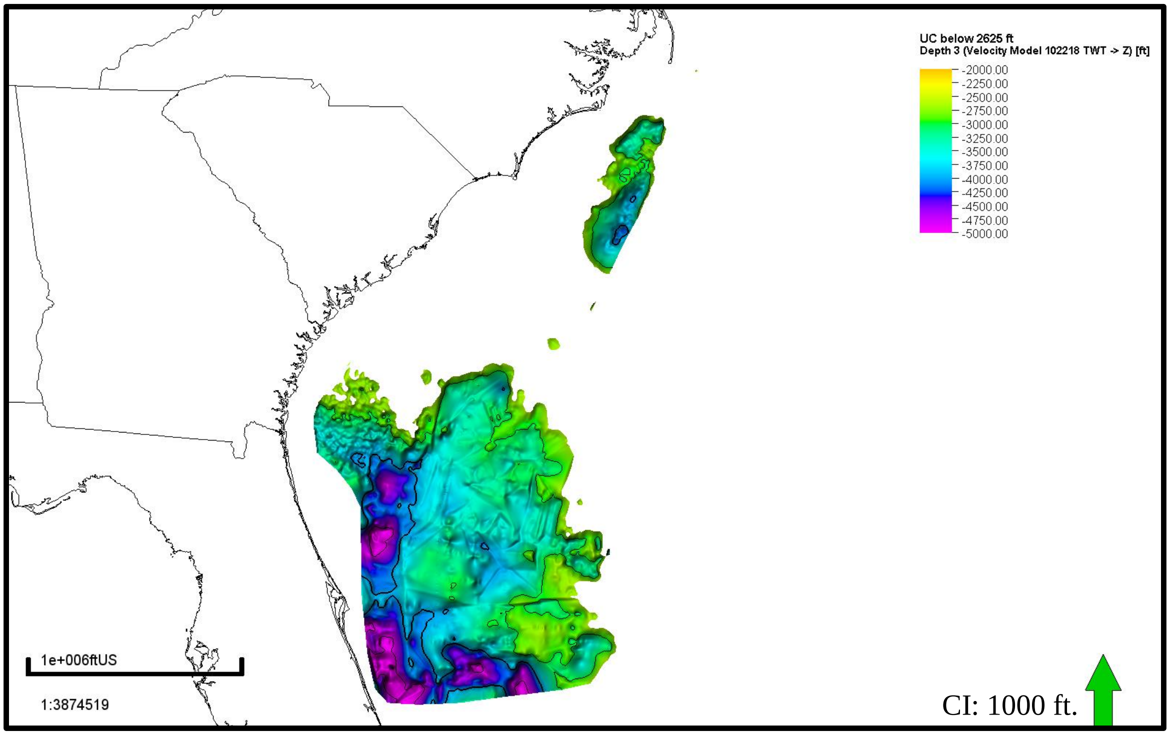

Figure 7.12: Upper Cretaceous surface exceeding 2625 ft. for supercritical CO_2 storage. 62% of the original surface meets this criterion.

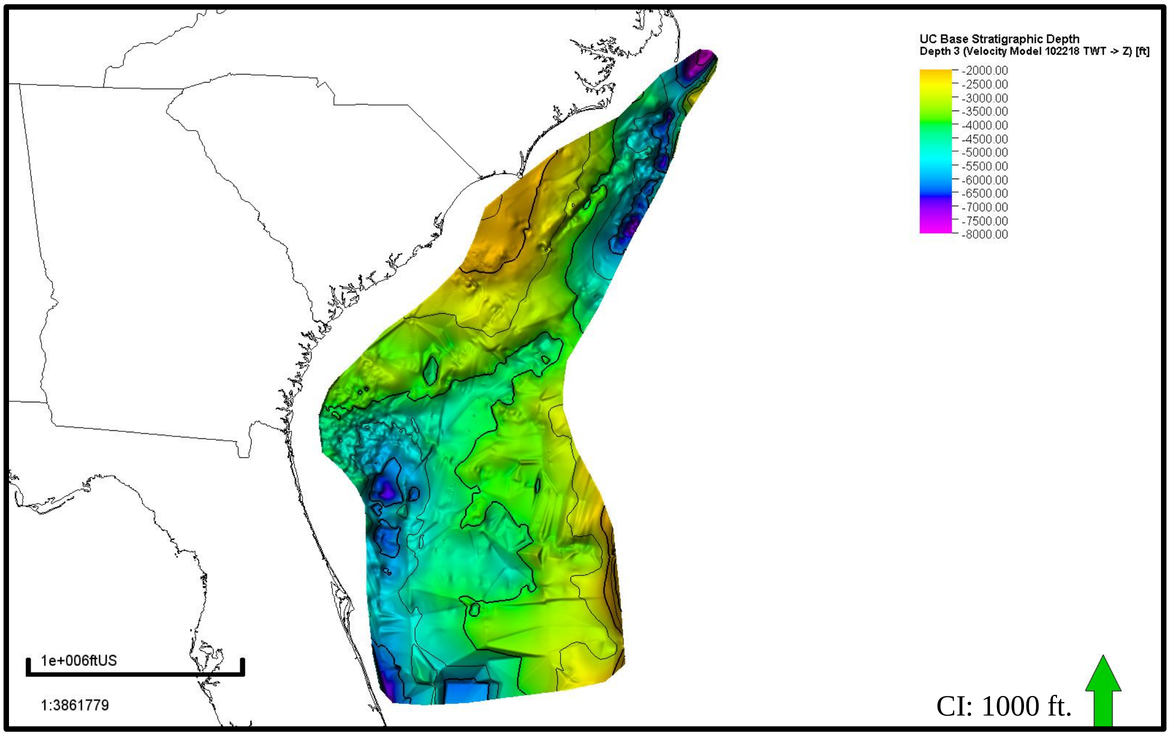

Figure 7.13: Lower Cretaceous stratigraphic depth surface

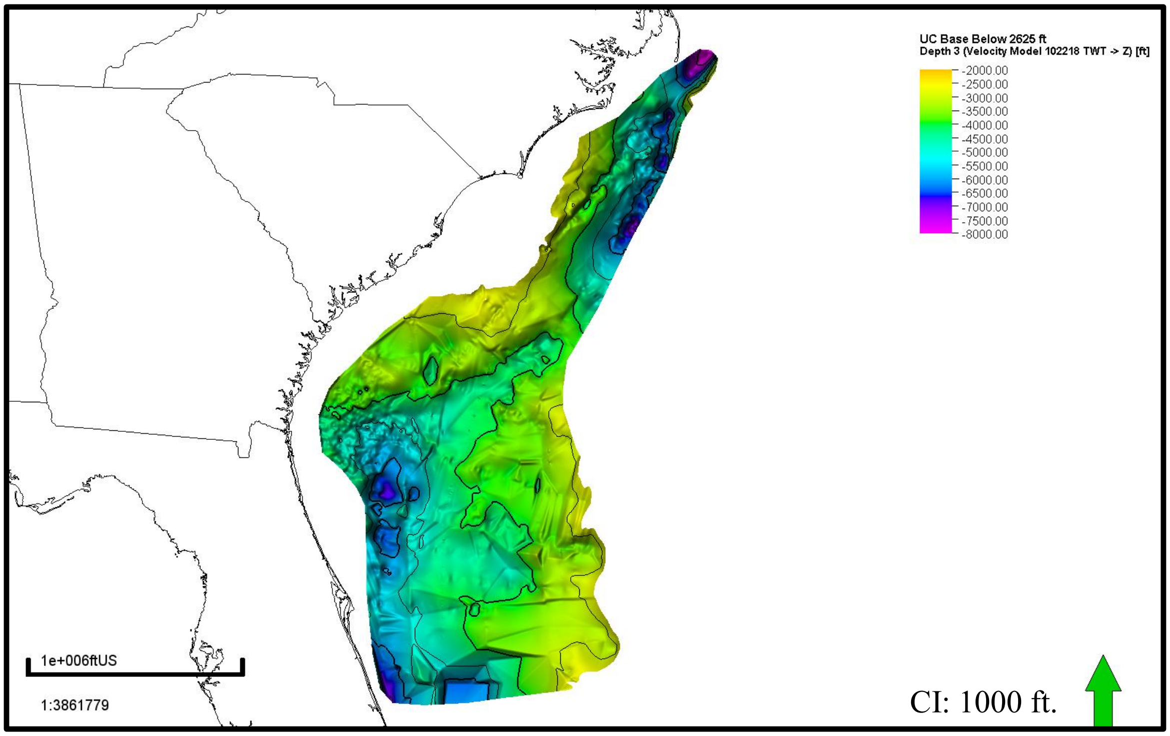

Figure 7.14: Lower Cretaceous surface exceeding 2625 ft. for supercritical CO_2 storage. 92% of the original surface meets this criterion.

CHAPTER 8

FUTURE IMPROVEMENTS

Through correspondence with BOEM, it was found that BOEM does not own the pre-stack seismic data for the stacked 2D seismic lines in the study area. Performing velocity analysis on pre-stack data for the BOEM dataset would provide a fantastic control on the accuracy of the velocity model. The pre-stack data could also have been used to add data points from lines with illegible stacking velocities published in .pdf files or lines without .pdf files. Alternative sources of publicly available pre-stack data were explored. Cruise IG1501, carried out by the Institute for Geophysics at the University of Texas at Austin in 1975, serves as the best publicly available pre-stack data set in the study area. Spanning the east coast from Northern Florida to North Carolina, this pre-stack data could add further data points to the model in addition to providing accuracy for areas with data points. The pre-stack data is unprocessed field data that needed various processing such as trace kills, muting, and NMO correction with seismic processing software (Figure 8.1). For instance, in several lines of the IG1501 cruise, at least 1 channel in a CDP needs to be killed. There is either too much noise or no signal in these situations.

However, the license for Landmark *SeisSpace ProMAX* at University of South Carolina was lost prior to completion of this thesis. Other options were explored to perform velocity analysis. The most successful of these options was *MATLAB*. Code developed by the CREWES Project at the Department of Geology and Geophysics of the University of Calgary provides a velocity analysis workflow. However, the raw, unprocessed data needs more robust processing software to make the data suitable for velocity analysis. NMO corrections were applied using the CREWES code, but the input parameters could not be edited. The semblance in the velocity analysis in *MATLAB* does not provide confident picks for velocities in each CDP gather. After velocity analysis, some CDP gathers have decreasing velocities with depth (Figure 8.2). This contradicts the COST GE-1 velocity data and data points from the published stacking velocities in the BOEM 2D seismic data set. With proper processing, these CDP gathers may produce more accurate velocity analysis results.

Additionally, there are further data points in .pdf files that can be added to the velocity model. Text recognition software was attempted on these files, but the files' resolution was not close to that required for the software. To add the data points, either advanced text recognition software or a large time commitment to manually enter the data points is required.

There are several .pdf files for lines in the seismic surveys and others that are illegible. Obtaining the original papers for these scanned files would be extremely helpful in adding further data points to the model. There may be higher quality resolution .pdf files in the BOEM database as well. All in all, there remains a plethora of stacking velocity data points that could not be used in the velocity model. Extracting these data points and adding them to the velocity model would be beneficial to filling in gaps without data in the study area.

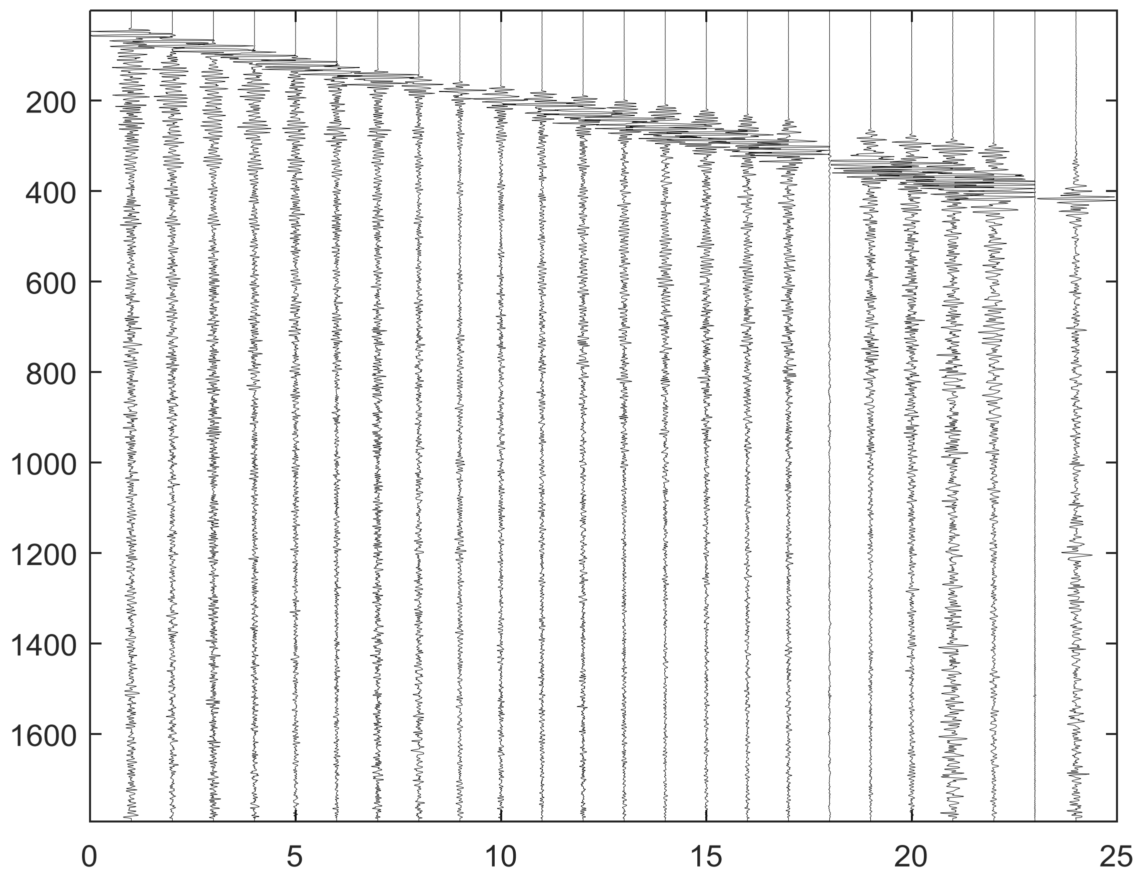

Figure 8.1: Example of CDP gather that would be improved with processing. CDP 281 from line se-3-28

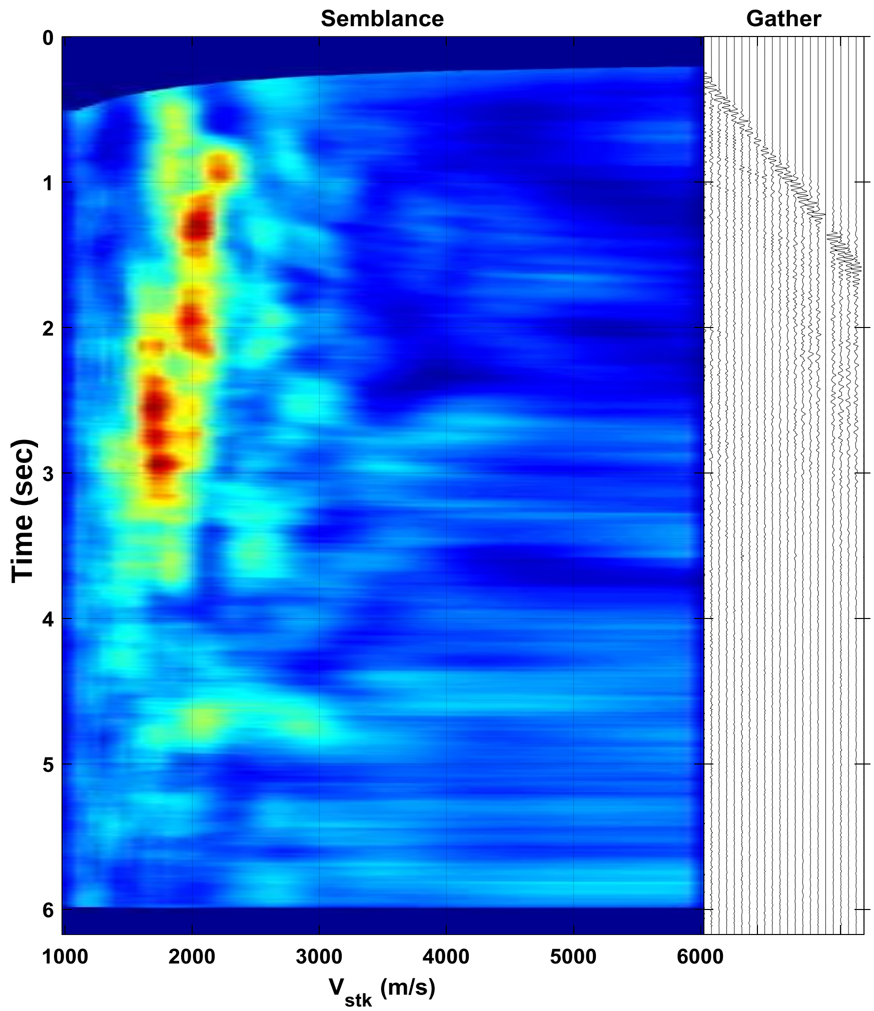

Figure 8.2: Example of CDP gather with poor semblance analysis results. From CDP 281 on line se-1-14. Semblance code by CREWES Project

CHAPTER 9

CONCLUSION

The accuracy of the velocity model is verified given the fact that the depth converted Upper Cretaceous and Paleozoic formations are similar to the formation tops in the COST GE-1 well. While improvements are always useful additions to the velocity model, the current model can be used in further research projects. The velocity model heavily contradicts the data points for formations from Hersey et al., 1959. With the well control added in 1975 after the study, it is apparent that the formation tops in Hersey et al., 1959 do not accurately reflect the geology. Therefore, further methods of control should be used when assessing the velocity model outside of the area of well control.

The velocity model workflow described in the hypothesis was verified. Determining the depths of stratigraphic units has several implications for the potential of CO_2 in the Southeastern United States Atlantic Continental Margin. It will allow the research team to estimate thicknesses and storage potentials for prospective CO_2 reservoirs. Knowledge of the depths of drilling targets will increase the chance of success if wells are drilled in the study area. Lastly, it ensures that potential CO_2 reservoirs are below the required 2,625 ft. for supercritical CO_2 storage. 62% of the top of the Upper Cretaceous formation exceeds this depth threshold. For the top of Lower Cretaceous, 92% of the surface exceed this threshold. Given these two discoveries, it is vital to continue further analyses on potential storage targets in these specified areas. As of now, it is apparent that the depth needed for supercritical CO_2 storage is present for the majority of our target formations in the study area.

REFERENCES

Almutairi, K. F., Knapp, C. C., Knapp, J. H., Terry, D. A. (2017) Assessment of Upper Cretaceous strata for offshore CO2 storage, Southeastern United States.

Dillon, W. P., & Popenoe, P. (1988). The Blake Plateau Basin and Carolina Trough. The Geology of North America, 2, 291-328.Dix, C. H. (1981). Seismic Prospecting for Oil. Boston: International Human Resources Development Corporation.

Dix, C. H. (1955). Seismic velocities from surface measurements. Geophysics, 20(1), 68-86.

Eiken, O., Ringrose, P., Hermanrud, C., Nazarian, B., Torp, T. A., & Høier, L. (2011). Lessons learned from 14 years of CCS operations: Sleipner, In Salah and Snøhvit. *Energy Procedia*, *4,* 5541-5548.

Hersey, J. B., Bunch, E. T., Wyrick, R. F., & Dietz, F. T. (1959). Geophysical investigation of the continental margin between Cape Henry, Virginia, and Jacksonville, Florida. *Geological Society of America Bulletin*, *70*(4), 437-466.

Hills, D. J., Pashin, J. C., & McIntyre-Redden, M. R. Southeast Offshore Storage Resource Assessment: Opportunities in the Eastern Gulf of Mexico for CO 2 Storage. In *AAPG Annual Convention and Exhibition*.

Katz, S., & Ewing, M. (1956). Seismic-Refraction Measurements in the Atlantic Ocean Part VII: Atlantic Ocean Basin, West of Bermuda. *Geological Society of America Bulletin*, *67*(4), 475-510.

Lindstrom, P. (2017, April 10). U.S. Energy Information Administration - EIA - Independent Statistics and Analysis. Retrieved September 01, 2017, from https://www.eia.gov/todayinenergy/detail.php?id=30712

Maher, J. C., & Applin, E. R. (1971). *Geologic framework and petroleum potential of the Atlantic Coastal Plain and Continental Shelf* (No. 659). US Govt. Print. Off.

Mitchell, K. L. (2013). Mitigation of Greenhouse Gases in the Southeast USA. In *Climate of the Southeast United States* (pp. 271-294). Island Press/Center for Resource Economics.

Neidell, N. S., & Taner, M. T. (1971). Semblance and other coherency measures for multichannel data. *Geophysics*, *36*(3), 482-497.

Pinet, P. R., & Popenoe, P. (1985). A scenario of Mesozoic-Cenozoic ocean circulation over the Blake Plateau and its environs. *Geological Society of America Bulletin*, *96*(5), 618-626.

Poag, C. W. (1991). Rise and demise of the Bahama-Grand Banks gigaplatform, northern margin of the Jurassic proto-Atlantic seaway. *Marine Geology*, *102*(1-4), 63-130.

Schrag, D. P. (2009). Storage of carbon dioxide in offshore sediments. *Science*, *325*(5948), 1658-1659.

Scholle, P. A. (1979). *Geological studies of the COST GE-1 well, United States South Atlantic outer continental shelf area*. US Department of the Interior, Geological Survey.

Sheridan, R. E., Drake, C. L., Nafe, J. E., & Hennion, J. (1966). Seismic-refraction study of continental margin east of Florida. *AAPG Bulletin*, *50*(9), 1972-1991.

Smyth, R. C., Hovorka, S. D., Meckel, T., Breton, C., Paine, J. G., Hill, G. R., ... & Li, W. (2007). Potential sinks for geologic storage of carbon dioxide generated in the Carolinas. *US Bureau of Econ Geol, summary report*, 1-pa14.

Yilmaz, Ö. (2001). Seismic data analysis: Processing, inversion, and interpretation of seismic data. Society of exploration geophysicists.